JACS
JOURNAL OF THE AMERICAN CHEMICAL SOCIETY
Article
pubs.acs.org/JACS

# Activation of Nitriles by Metal Ligand Cooperation. Reversible Formation of Ketimido- and Enamido-Rhenium PNP Pincer Complexes and Relevance to Catalytic Design

Matthias Vogt,[†,§] Alexander Nerush,[†,§] Mark A. Iron,[‡] Gregory Leitus,[‡] Yael Diskin-Posner,[‡] Linda J. W. Shimon,[‡] Yehoshoa Ben-David,[†] and David Milstein*[,†]

[†]Department of Organic Chemistry, and [‡]Department of Chemical Research Support, The Weizmann Institute of Science, Rehovot 76100, Israel

Supporting Information

**ABSTRACT:** The dearomatized complex *cis*-[Re(PNP$^{tBu}$*)-(CO)$_2$] (**4**) undergoes cooperative activation of C≡N triple bonds of nitriles via [1,3]-addition. Reversible C−C and Re−N bond formation in **4** was investigated in a combined experimental and computational study. The reversible formation of the ketimido complexes (**5**−**7**) was observed. When nitriles bearing an alpha methylene group are used, reversible formation of the enamido complexes (**8** and **9**) takes place. The reversibility of the activation of the nitriles in the resulting ketimido compounds was demonstrated by the displacement of *p*-CF$_3$-benzonitrile from *cis*-[Re(PNP$^{tBu}$−N=CPh$^{pCF3}$)(CO)$_2$] (**6**) upon addition of an excess of benzonitrile and by the temperature-dependent [1,3]-addition of pivalonitrile to complex **4**. The reversible binding of the nitrile in the enamido compound *cis*-[Re(PNP$^{tBu}$−HNC=CHPh)(CO)$_2$] (**9**) was demonstrated via the displacement of benzyl cyanide from **9** by CO. Computational studies suggest a stepwise activation of the nitriles by **4**, with remarkably low activation barriers, involving precoordination of the nitrile group to the Re(I) center. The enamido complex **9** reacts via *β*-carbon methylation to give the primary imino complex *cis*-[Re(PNP$^{tBu}$−HN=CC(Me)Ph)(CO)$_2$]OTf **11**. Upon deprotonation of **11** and subsequent addition of benzyl cyanide, complex **9** is regenerated and the monomethylation product 2-phenylpropanenitrile is released. Complexes **4** and **9** were found to catalyze the Michael addition of benzyl cyanide derivatives to *α*,*β*-unsaturated esters and carbonyls.

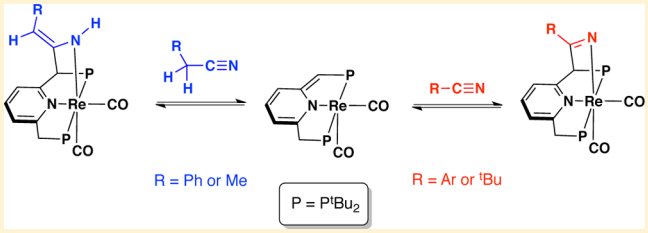


## INTRODUCTION

Metal−ligand cooperation (MLC), in which both the metal center and a ligand undergo bond formation and cleavage without a formal change in the oxidation state of the metal, has become a powerful tool in bond activation chemistry and "green" catalysis.[1−7] In this regard, transition metal (TM) complexes with pyridine- and acridine-based LNL′-type pincer ligands are versatile in bond activation processes (for instance, S−H,[8,9] N−H,[10,11] O−H,[12] H−H,[13−15] and C−H[15−19] single bonds). Among these examples, the aromatization/dearomatization sequence of the pyridine-based pincer ligand is the key step for MLC-promoted substrate activation. It is involved in recently developed, atom-economic catalytic reactions, specifically the acceptorless dehydrogenative coupling (DHC) of alcohols to esters,[20−23] the oxidation of alcohols to carboxylic acids using water as oxidant,[24] DHC of alcohols and amines to amides,[25−27]imines,[28] or pyrroles,[29,30] the coupling of nitriles with amines under hydrogen pressure to form imines,[23] the synthesis of primary amines directly from alcohols and ammonia,[31,32] the hydrogenation of esters to alcohols,[33,34] the direct hydrogenation of amides to alcohols and amines,[35] the hydrogenation of organic carbonates/cabamates[36] or urea derivatives[37] to methanol, and the hydrogenation of $CO_2$.[38−41] Recently, we and others have reported on C−C bond formation between the *exo*-cyclic methine carbon of our dearomatized pincer complexes and substrates bearing C=O double bonds, specifically $CO_2$[42−44] and aldehydes.[45] MLC plays a key role in these substrate activations, and we found evidence for a concerted C−C and Ru−O bond formation when $CO_2$ binds to **A** (Scheme1). Along these lines, we now report on the activation of C≡N triple bonds (i.e., nitriles) triggered via MLC in a rhenium(I) PNP-pincer type complex (Scheme 2). In contrast to the well-established ruthenium pincer chemistry, rhenium PNP pincer-type complexes are sparsely discussed in the literature. A few amino-bisphosphino rhenium pincer compounds were previously reported,[46−48] in studies aimed at radio pharmaceutical applications.[49−52] The cleavage of dihydrogen promoted by MLC was shown by Gusev and co-workers in the amido-bisphosphine complexes of [ReH(NO)(N(C$_2$H$_4$PR$_2$)$_2$] (R = $^t$Bu or $^i$Pr).[53] Pyridine-based PNP rhenium pincer complexes are particularly rare. Walton and co-workers prepared rhenium(III)-complexes with such a ligand, furnishing Re−Re multiple bonds.[54,55] Recently,

**Received:** July 14, 2013
**Published:** November 5, 2013

   dx.doi.org/10.1021/ja4071859 | J. Am. Chem. Soc. 2013, 135, 17004−17018

**Scheme 1. Metal–Ligand Cooperative Activation of C═O Double Bonds and the Novel Activation of C≡N Triple Bonds via M–N(O) and C–C Bond Formation**

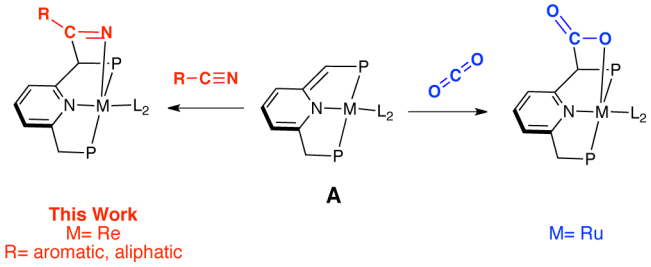


**Scheme 2. Synthesis of the Dearomatized Complex 4 and Subsequent Reactions with Nitriles Lacking an α-Methylene Carbon (5–7) and with Aliphatic Nitriles (8, 9)**

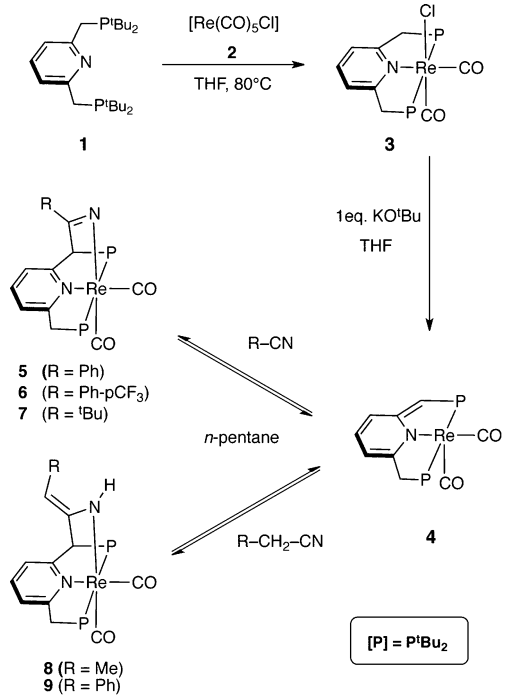


structurally well-defined Re complexes have been reported by Berke et al. and Klankermayer et al. as highly efficient catalyst for (transfer) hydrogenation reactions.[56−60]

This work involves the synthesis of *cis*-[Re(PNP$^{tBu}$)(CO)$_2$Cl] (**3**, PNP$^{tBu}$ = 2,6-bis(di-*tert*-butylphosphinomethyl)-pyridine, Scheme 2), a versatile rhenium(I) starting material, which is readily deprotonated to give the dearomatized species [Re(PNP$^{tBu}$*)(CO)$_2$] (**4**, the asterisk indicates a dearomatized ligand). Significantly, complex **4** reacts with nitriles via reversible C–C and Re–N bond formation to give [1,3]-addition products (Scheme 2). This unprecedented mode of activation of nitriles readily leads to ketimido and enamido ligands and to catalysis based on this unusual mode of metal–ligand cooperation.

## RESULTS AND DISCUSSION

Complex **3** is readily prepared by the reaction of commercially available [Re(CO)$_5$Cl] (**2**) and 2,6-bis(di-*tert*-butylphosphinomethyl)pyridine (PNP$^{tBu}$, **1**) in THF at 80 °C (Scheme 2). The $^{31}$P{$^1$H} NMR spectrum of **3** exhibits a characteristic singlet at 68.8 ppm indicating two chemically equivalent phosphorus nuclei. The $^1$H NMR spectrum has two resonances for the pyridine backbone in the aromatic regime: a virtual triplet ($^3J_{HH}$ = 7.8 Hz) at 7.62 ppm assigned to the *para*-C*H* proton and a doublet at 7.36 ppm ($^3J_{HH}$ = 7.8 Hz), integrating to two protons, for both *meta*-C*H* protons. The IR spectrum exhibits strong absorptions characteristic of the CO ligands at 1816 and 1900 cm$^{-1}$ with a relative intensity of 1:1, indicating an angle of 90° between both ligands. Large single crystals of the bright yellow **3** were obtained from a *n*-pentane-layered THF solution. The molecular structure derived from an X-ray diffraction study is shown in Figure 1. (Selected bond lengths for all X-ray structures are given in Table 1.) The tridentate PNP$^{tBu}$ ligand binds to the Re(I) center in a meridonal manner. The two CO ligands bind mutually *cis*, and the axial chloride completes the octahedral coordination sphere.

Upon addition of KO$^t$Bu, the yellow THF solution of **3** turns instantly deep green. Extraction with *n*-pentane and subsequent slow evaporation of the solvent gives the dearomatized complex **4** as large green crystals. The $^{31}$P{$^1$H} NMR spectrum of **4** indicates a reduced symmetry with an AB-spin system, suggesting that the two phosphorus nuclei are inequivalent, with doublets at 68.9 and 74.7 ppm ($^2J_{PP}$ = 145 Hz). Likewise, the $^1$H NMR spectrum of **4** has three signals for the pyridine protons, signifying the reduction in symmetry, specifically the loss of the mirror plane perpendicular to the pyridine ring. These signals (see Experimental Section for details) are shifted to lower frequencies, indicative of a dearomatized PNP ligand. Deprotonation of the *exo*-cyclic methylene group results in two pincer-"arm" resonances in the $^1$H NMR spectrum: a doublet at 2.74 ppm ($^2J_{HP}$ = 9.2 Hz, 2H) for the two equivalent C$H_2$ protons and a broad singlet at 4.06 ppm (1H) for the methine C*H* proton. There is only one signal in the carbonyl regime of the $^{13}$C{$^1$H} NMR spectrum, suggesting the presence of a symmetry plane through the PNP pyridine ring. This indicates a trigonal bipyramidal geometry or rapid conversion on the NMR time scale of two equivalent square pyramidal structures in solution. However, dynamic exchange in solution could not be concluded from phase-sensitive 2D $^1$H–$^1$H NOESY NMR spectroscopy. The $^1$H NMR resonances of the methylene C$H_2$ and the methine C*H* protons do not share significant cross-peaks, which would indicate mutual chemical exchange due to interconversion of two pyramidal structures.

However, the IR spectrum of crystalline **4** in a KBr pellet shows two intense bands at 1827 and 1906 cm$^{-1}$ with a relative intensity ratio of 1:1, implying a bond angle of 90°. Single crystals of **4** suitable for X-ray diffraction studies were obtained from a concentrated solution in *n*-pentane (Figure 1). The structure reveals a distorted square pyramidal geometry around

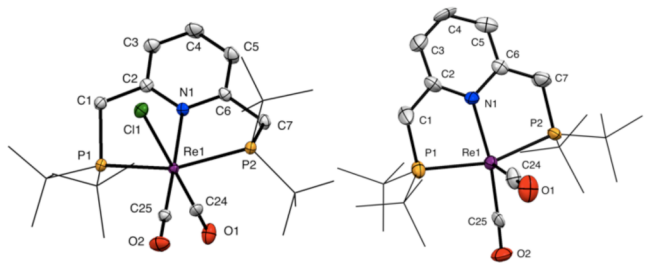


**Figure 1.** ORTEP diagram of [Re(PNP$^{tBu}$)(CO)$_2$Cl] (**3**, left) and [Re(PNP$^{tBu}$*)(CO)$_2$] (**4**, right) with ellipsoids at 50% probability. The P(*tert*-butyl)$_2$ groups are drawn as wire-frames, and hydrogen atoms are omitted for clarity. Selected bond lengths are given in Table 1.


dx.doi.org/10.1021/ja4071859 | J. Am. Chem. Soc. 2013, 135, 17004–17018

**Table 1. Selected Bond Lengths for the Crystal Structures of Complexes 3−5 and 7−11**

| bond lengths (Å) | 3 | 4 | 5 | 7 | 8 | 9 | 10 | 11 |
|---|---|---|---|---|---|---|---|---|
| Re1−N1 | 2.183(3) | 2.135(7) | 2.183(4) | 2.186(4) | 2.178(4) | 2.174(2) | 2.195(4) | 2.171(2) |
| Re1−N2 | | | 2.191(5) | 2.168(4) | 2.173(4) | 2.173(3) | 2.232(4) | 2.168(2) |
| Re1−C24 | 1.899(4) | 1.866(10) | 1.902(6) | 1.897(5) | 1.889(5) | 1.886(3) | 1.888(5) | 1.907(3) |
| Re1−C25 | 1.900(3) | 1.901(9) | 1.898(6) | 1.906(5) | 1.910(5) | 1.909(3) | 1.897(6) | 1.904(2) |
| Re1−P1 | 2.4383(8) | 2.417(2) | 2.414(1) | 2.394(1) | 2.403(1) | 2.413(1) | 2.407(1) | 2.4107(9) |
| Re1−P2 | 2.4434(8) | 2.399(2) | 2.404(1) | 2.409(1) | 2.413(1) | 2.4139(9) | 2.454(1) | 2.4113(9) |
| C1−C2 | 1.505(4) | 1.402(12) | 1.494(8) | 1.514(6) | 1.487(6) | 1.502(5) | 1.518(6) | 1.515(3) |
| C2−C3 | 1.389(4) | 1.425(12) | 1.393(8) | 1.391(6) | 1.396(6) | 1.399(4) | 1.362(8) | 1.382(3) |
| C3−C4 | 1.375(5) | 1.355(13) | 1.376(9) | 1.394(8) | 1.368(7) | 1.378(5) | 1.396(8) | 1.383(3) |
| C4−C5 | 1.390(5) | 1.407(15) | 1.373(10) | 1.366(8) | 1.400(6) | 1.384(5) | 1.382(8) | 1.377(4) |
| C5−C6 | 1.388(4) | 1.365(14) | 1.387(8) | 1.390(6) | 1.388(6) | 1.389(4) | 1.392(8) | 1.388(3) |
| C6−C7 | 1.515(4) | 1.532(15) | 1.498(8) | 1.501(7) | 1.513(6) | 1.507(4) | 1.501(7) | 1.505(3) |
| N1−C2 | 1.358(4) | 1.409(11) | 1.356(7) | 1.358(6) | 1.355(6) | 1.351(4) | 1.359(6) | 1.360(3) |
| N1−C6 | 1.363(4) | 1.388(11) | 1.365(7) | 1.360(6) | 1.370(6) | 1.357(4) | 1.357(6) | 1.354(3) |
| P1−C1 | 1.855(3) | 1.772(9) | 1.878(5) | 1.874(4) | 1.866(5) | 1.881(3) | 1.886(5) | 1.900(2) |
| P2−C7 | 1.856(3) | 1.796(11) | 1.858(6) | 1.863(5) | 1.881(5) | 1.861(3) | 1.854(5) | 1.858(2) |
| N2−C26 | | | 1.260(7) | 1.266(6) | 1.348(6) | 1.349(4) | 1.288(7) | 1.282(3) |
| C26−C27 | | | 1.502(7) | 1.545(6) | 1.409(6) | 1.388(4) | 1.488(7) | 1.511(3) |
| C26−C1 | | | 1.574(8) | 1.560(6) | 1.543(6) | 1.545(4) | 1.522(6) | 1.515(3) |
| X−Y | 2.5238(8)[a] | | | | | | 1.478(6)[b] | 1.535(3)[c] |

[a]Re1−Cl1. [b]N2−C34. [c]C27−C28.

the Re(I) center. The angle between the two CO ligands (C24−Re1−C25) is 86°, and the angles between the pyridine ligand and the CO moieties are 115° (N1−Re−C24) and 159° (N1−Re1−C25). Selected bond lengths for all X-ray structures are given in Table 1.

**Reaction with Nitriles.** Complex **4** reacts in *n*-pentane solution with aromatic and aliphatic nitriles (Scheme 2). Upon addition of benzonitrile (PhCN), 4-(triflouromethyl)-benzonitrile ($^{p\mathrm{CF3}}$PhCN), or pivalonitrile ($^{t}$BuCN), ketimide complexes **5**−**7** are formed. Remarkably, the C≡N triple bond binds reversibly to give the [1,3]-addition product via C−C and Re−N bond formation. Transition metal ketimide complexes have drawn special attention as they can function as both $\sigma$- and $\pi$-donors. They are stabilizing ligands in highly oxidized TM complexes[61−64] and for actinide metal centers.[65,66] They have been reported as ligands promoting strong M−M interactions[67] and have found application as olefin polymerization catalysts with group four metal centers.[68−71]

The ketimide complexes *cis*-[Re(PNP$^{t\mathrm{Bu}}$−N=CPh)(CO)$_2$] (**5**) and *cis*-[Re(PNP$^{t\mathrm{Bu}}$−N=CPh$^{p\mathrm{CF3}}$)(CO)$_2$] (**6**) have AB-spin systems in their $^{31}$P{$^{1}$H} NMR spectra at chemical shifts characteristic for aromatized PNP ligand systems (86.6 and 128.2 ppm with $^{2}J_{\mathrm{PP}}$ = 193.8 Hz for **5**, and 86.6 and 129.4 ppm with $^{2}J_{\mathrm{PP}}$ = 191.9 Hz for **6**). This is also reflected in the $^{1}$H NMR chemical shifts of the pyridine hydrogen atoms, which are in the aromatic regime (see the Experimental Section). For the pincer C*H*$_2$ arm, there are two sets of doublets of doublets with large geminal couplings ($^{2}J_{\mathrm{HH}}$ = 15.50 Hz for **5** and **6**) and smaller phosphorus couplings ($^{2}J_{\mathrm{HP}}$ = 5.00 and 9.00 Hz for **5** and **6**, respectively). The C*H* methine "arm" appears as a doublet with a small phosphorus coupling (details in the Experimental Section).

The observed [1,3]-addition of nitriles to form complexes **5**−**7** is a novel route for the synthesis of ketimido compounds, complementary to those commonly used.[68] This reactivity mode is fully reversible. For instance, when a large excess of benzonitrile is added to a solution of **6** in $C_6D_6$, the formation of **5** and free $^{p\mathrm{CF3}}$Ph−CN is observed. An equilibrium constant of $^{298}K_{\mathrm{eq}}$ = 0.021 was determined for the reaction **6** + Ph−CN ⇌ **5** + $^{p\mathrm{CF3}}$Ph−CN (Scheme 3), indicating the higher thermodynamic stability of the adduct of the electron poor nitrile.

The reversibility of nitrile binding by MLC is best demonstrated with $^{t}$BuCN. Reacting the deep green *n*-pentane solution of **4** at −38 °C with an excess of $^{t}$BuCN produces large red crystals after 24 h. The $^{1}$H and $^{31}$P{$^{1}$H} NMR spectra of a solution of the crystals in toluene-$d_8$ at room temperature show very broad signals. Upon stepwise cooling to −65 °C, these resonances broaden further and eventually collapse while at the same time sharp resonances appear (Figure 2), consistent with

**Scheme 3. Reversible Binding of Nitriles to [Re(PNP$^{t\mathrm{Bu}}$*)(CO)$_2$] (4)[a]**

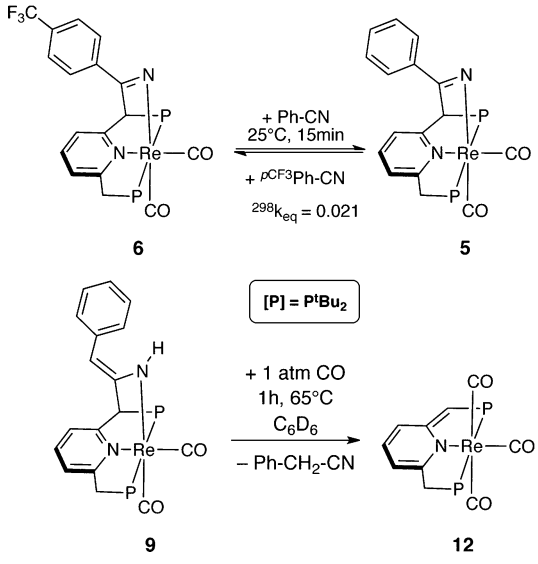


[a]Top: Displacement of $^{p\mathrm{CF3}}$PhCN from **6** by an excess of PhCN. Bottom: Displacement of PhCH$_2$CN from **9** by CO.


dx.doi.org/10.1021/ja4071859 | J. Am. Chem. Soc. 2013, 135, 17004−17018

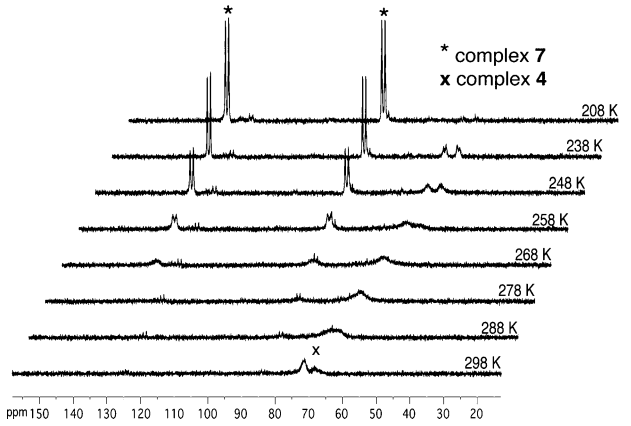


**Figure 2.** Sections of the variable-temperature $^{31}P\{^{1}H\}$ NMR spectra (298−208 K) of **7** in toluene-$d_8$.

the formation of complex **7**; see the Experimental Section for full spectral assignments. Characteristically, the solution of **7** is intense red at lower temperatures and deep green, typically observed for solutions of the dearomatized complex **4**, at ambient temperature.[72]

Single crystals for complexes **5** and **7** were obtained from concentrated *n*-pentane solutions. In the case of **7**, the presence of excess $^{t}$BuCN was necessary. The molecular structures derived from single-crystal X-ray diffraction analyses are shown in Figure 3. The structures of **5** and **7** are distorted octahedra around the Re(I) centers with both CO ligands in mutually *cis* positions. The ketimido ligands are bound in axial positions and show characteristic N=C double bond lengths (N2−C26 = 1.26 Å in **5**; N2−C26 = 1.27 Å in **7**) comparable to those of previously reported ketimido complexes.[61,62,73,74] The newly formed C−C bond between the nitrile substrate and the *exo*-cyclic carbon atom of the pincer ligand (C1−C26) is slightly elongated by ∼0.06 Å (C1−C26 = 1.57 Å in **5**; C1−C26 = 1.56 Å in **7**) relative to the C6−C7 single bond. The Re1−N2 bond lengths to the ketimide ligand (Re1−N2 = 2.19 Å in **5**; Re1−N2 = 2.17 Å in **7**) are consistent with previously reported complexes (e.g., in manganese complexes).[67]

Substrates with a nitrile moiety adjacent to a methylene $CH_2$ group, such as propiononitrile and benzyl cyanide, give the enamido complexes *cis*-[Re(PNP$^{tBu}$−HNC=CHMe)(CO)$_2$] (**8**) and *cis*-[Re(PNP$^{tBu}$−HNC=CHPh)(CO)$_2$] (**9**), respectively (Scheme 2). Complexes **8** and **9** are tautomers of the corresponding ketimides via a formal [1,3]-proton shift. The $^{31}P\{^{1}H\}$ NMR spectra ($C_6D_6$, 25 °C) show the expected AB-spin system with doublet resonances at 84.8 and 95.6 ppm ($^{2}J_{PP}$ = 191.0 Hz) for complex **8** and 82.9 and 98.9 ppm ($^{2}J_{PP}$ = 186.6 Hz) for **9**, indicative of two phosphorus nuclei in dissimilar chemical environments.[75]

The $^{1}$H NMR spectra show the characteristic resonances for the olefinic-C*H* protons for the enamido moieties: a quartet at 4.25 ppm ($^{3}J_{HH}$ = 6.50 Hz) in **8** and a singlet at 5.32 ppm in **9**. The characteristic amido-N*H* proton is detected as a broad singlet at 2.38 ppm in **8** and at 4.65 ppm in **9**. The aromatic resonances for the pyridine backbone in **8** and **9** are observed; for full assignment, see the Experimental Section.

The reversible binding of benzyl cyanide to **4** was demonstrated. Upon exposure of the coordinatively saturated complex **9** in $C_6D_6$ to 1 atm of CO, the red solution slowly changes to yellow, and the dearomatized tricarbonyl complex *mer*-[Re(PNP$^{tBu}$*)(CO)$_3$] (**12**) is formed together with detected free $PhCH_2CN$ (Scheme 3). This transformation can be followed by $^{31}P\{^{1}H\}$ NMR spectroscopy (Figure 4): after the addition of CO, complex **12** starts to form, and this transformation is completed after 1 h at 65 °C.

The presence of the enamido moiety in **8** and **9** is supported by a single-crystal X-ray diffraction study (Figure 5, Table 1). The enamido moiety is characterized by a short C=C double bond between C26 and C27 (1.41 Å in **8** and 1.39 Å in **9**). Both structures have the amido ligand in an axial position with the N2−C26 distances corresponding to N−C single bonds adjacent to an sp$^2$-carbon atom (N2−C26 = 1.35 Å in **8** and **9**). The newly formed C1−C26 bonds between the pincer arm and enamido moiety are in the range of C−C single bonds (C1−C26 = 1.54 Å in **8**; C1−C26 = 1.55 Å in **9**). The rhenium−nitrogen bonds (Re1−N2 = 2.17 Å in **8** and **9**) are comparable to those found in ketimides complexes **5** and **7**. The rhenium(I) centers in both complexes have distorted octahedral coordination spheres formed by the axial amido moiety, two mutually *cis* CO ligands, and the meridional tridentate PNP$^{tBu}$ pincer ligand.

**DFT Calculations.** To better understand the mechanism by which this MLC activation occurs, the system was studied computationally using density functional theory (DFT) at the

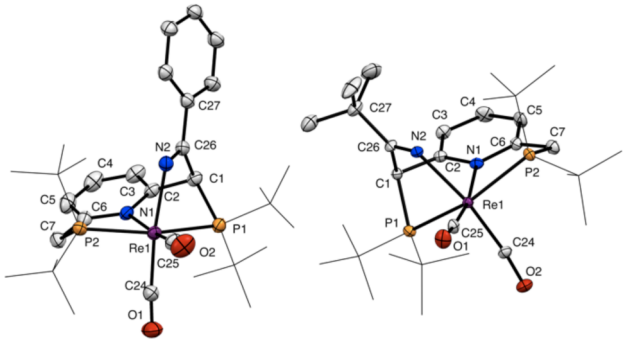


**Figure 3.** ORTEP diagram of *cis*-[Re(PNP$^{tBu}$−N=CPh)(CO)$_2$] (**5**, left) and *cis*-[Re(PNP$^{tBu}$−N=C$^{t}$Bu)(CO)$_2$] (**7**, right) with ellipsoids at 30% probability. The P(*tert*-butyl)$_2$ groups are drawn as wire-frames, and hydrogen atoms are omitted for clarity. Selected bond lengths are given in Table 1.

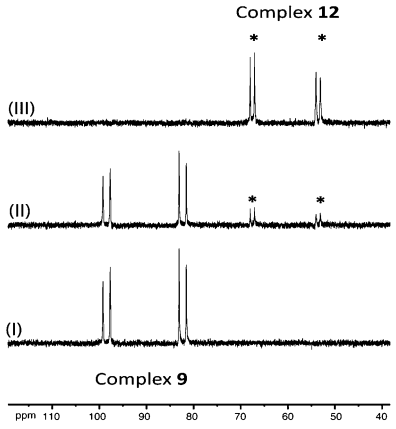


**Figure 4.** Sections of the $^{31}P\{^{1}H\}$ NMR spectra of **9** in $C_6D_6$ (bottom, I), under 1 atm of CO for 15 min "(middle, II, * indicates resonances correlated to **12**), and under 1 atm CO at 65 °C for 1 h forming of **12** (top, III).


dx.doi.org/10.1021/ja4071859 | J. Am. Chem. Soc. 2013, 135, 17004−17018

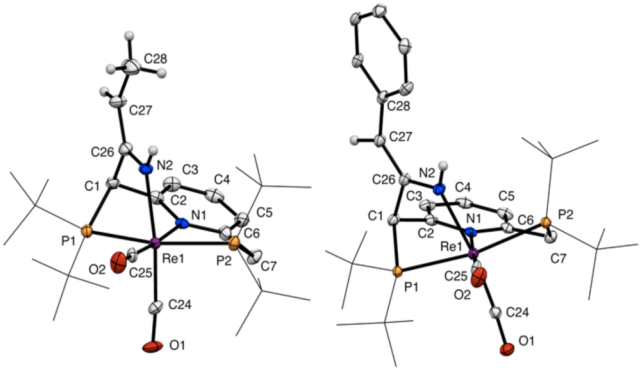


**Figure 5.** ORTEP diagram of *cis*-[Re(PNP$^{tBu}$–HNC═CHMe)(CO)$_2$] (**8**, left) and *cis*-[Re(PNP$^{tBu}$–HNC═CHPh)(CO)$_2$] (**9**, right) with ellipsoids at 30% probability. The P(*tert*-butyl)$_2$ groups are drawn as wire-frames, and hydrogen atoms, except partially for the enamido moieties, are omitted for clarity. Selected bond lengths are given in Table 1.

SMD(*n*-pentane)-DSD-PBEP86/cc-pV(D+d)Z//DF-PBE+d$_{v2}$/SDD(d) level of theory (see the Computational Methods section for full details). Energies reported herein are $\Delta G_{298,sol}$ relative to **4** + R–CN (R = Et, $^t$Bu, Ph, PhCH$_2$, $^{p^{CF3}}$Ph, $^{p^{NH2}}$Ph). In a previous study, the reaction of a related ruthenium complex with CO$_2$ was investigated, and a concerted CO$_2$ addition mechanism was found where the Ru–O and C–C bonds are formed in one concerted step.[42]

The reaction with a number of nitriles was examined, and the reaction profiles are shown in Figure 6. A concerted mechanism was considered here, but the transition state found (Figure 7) is associated with a Re–nitrile coordination complex prior to activation. This coordination complex is slightly higher in energy than the separated species and thus unlikely to be observed experimentally. Nonetheless, this complex and the subsequent transition state are sufficiently low to afford a very rapid reaction (reaction barriers are all less than 15 kcal/mol).

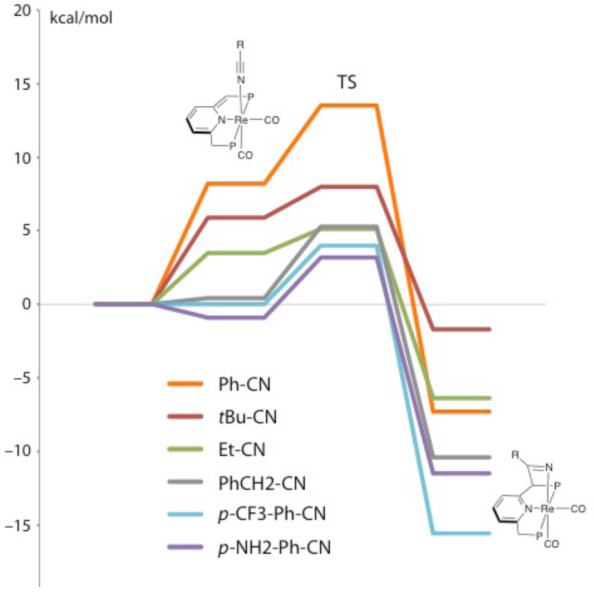


**Figure 6.** Reaction profiles ($\Delta G_{298,sol}$, kcal/mol, at the SMD(*n*-pentane)-DSD-PBEP86/cc-pV(D+d)Z//DF-PBE+d$_{v2}$/SDD(d) level of theory) for the reactions of **4** with various nitriles.

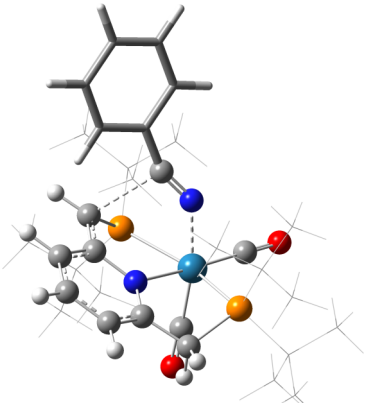

**Figure 7.** Transition state for the reaction of [Re(PNP$^{tBu}$*)(CO)$_2$] (**4**) with PhC≡N; the transition states for the other nitriles are similar in appearance. The P(*tert*-butyl)$_2$ groups are drawn as wire-frames.

It is interesting to note that when PhCN is substituted in the *para* position by either an electron-withdrawing (e.g., CF$_3$) or an electron-donating (e.g., NH$_2$, not considered experimentally) group, the products and associated transition states are lower in energy than for PhCN. The low barrier and reaction energy for the reaction with $^t$BuCN indicates a fast reversible reaction. At room temperature, broad signals are observed in the $^1$H and $^{31}$P{$^1$H} NMR spectra, consistent with a rapid equilibrium (on NMR time scale) between reactants and product **7**. Upon cooling, only the sharp resonances of **7** are observed. Likewise, with $^{p^{CF3}}$PhCN, only product **6** is observed by NMR spectroscopy, but the relatively low reverse barrier ($\Delta G_{298}^{\ddagger}$ = 19.6 kcal/mol) indicates that the exchange is possible, as experimentally observed when a large excess of PhCN is added to **7**. Two nitriles, EtCN and PhCH$_2$CN, have an $\alpha$-hydrogen and can thus tautomerize to the enamide complexes **8** and **9**, respectively. It is not unreasonable to assume that the reaction initially proceeds via the corresponding ketimide complex. It was found that in the case of the PhCH$_2$CN, the enamide complex is lower in energy, while in the case of EtCN the two complexes are, within the DFT error estimate, practically isoergonic (Table 2.).

There are examples of iron(II) complexes with coordinated 1,3-diimine and nitrile ligands. Upon addition of base, both ligands react giving C–C bond formation.[76,77] In line with our mechanistic considerations, an intramolecular mechanism has been proposed for these systems entailing proton abstraction by the base from the central methylene carbon of the 1,3-diimine and subsequent nucleophilic attack at the $\alpha$-carbon of

**Table 2. Energies ($\Delta G_{298,sol}$, kcal/mol, at the SMD(*n*-pentane)-DSD-PBEP86/cc-pV(D+d)Z//DF-PBE+d$_{v2}$/SDD(d) Level of Theory) of the Intermediates, Transition States, and Products of the Reactions of 4 with Various Nitriles**

| nitrile | RCN–[Re] | TS | ketimide | enamide |
|---|---|---|---|---|
| PhCN | 8.2 | 13.5 | −7.3 | −[a] |
| $^t$BuCN | 5.9 | 8.0 | −1.7 | −[a] |
| $^{p^{CF3}}$PhCN | 0.0 | 4.0 | −15.6 | −[a] |
| $^{p^{NH2}}$PhCN | −0.9 | 3.2 | −11.5 | −[a] |
| EtCN | 3.5 | 5.1 | −6.4 | −6.1 |
| PhCH$_2$CN | 0.4 | 5.3 | −10.4 | −13.1 |

[a]Not applicable.


dx.doi.org/10.1021/ja4071859 | J. Am. Chem. Soc. 2013, 135, 17004–17018

the coordinated nitrile. Reprotonation of the ketimido moiety, bound to the Fe center, gives the final imino product. Electron-withdrawing groups attached to the $\alpha$-carbon of the nitrile accelerate the reaction.[78]

**Reaction with Strong Electrophiles.** Complexes **6** and **9** were reacted with methyl triflate in benzene (Scheme 4). The ketimide complex **6** undergoes methylation of the ketimide nitrogen atom to form the corresponding cationic imino complex *cis*-[Re(PNP$^{tBu}$–N(Me)=CPh$^{pCF3}$)(CO)$_2$]OTf (**10**). The $^{31}$P{$^1$H} NMR in acetone-$d_6$ exhibits an AB-spin system consisting of two doublets with a large peak separation (89.3 and 149.7 ppm, $^2J_{PP}$ = 165.0 Hz). The $^1$H NMR spectrum has a characteristic sharp singlet resonance with an integration value equal to three protons for the introduced *N*-methyl group at 3.97 ppm. In contrast, the enamido complex **9** reacts with methyl triflate to form the cationic primary imine compound *cis*-[Re(PNP$^{tBu}$–HN=C–CH(Me)Ph)(CO)$_2$]OTf (**11**) by methylation of the $\alpha$-carbon atom (Scheme 4). The $^1$H NMR spectrum of **11** in CD$_3$CN has a doublet resonance assigned to the introduced methyl group at 1.47 ppm ($^3J_{HH}$ = 7.0 Hz). Significantly, the C=N*H* proton resonance is detected as a broad singlet at 9.96 ppm. The $^{31}$P{$^1$H} NMR spectrum has the expected AB-spin system with doublets at 88.9 and 147.5 ppm ($^2J_{PP}$ = 164.4 Hz). The IR spectra (KBr pellet) show two strong absorption bands in a 1:1 ratio at 1924 and 1866 cm$^{-1}$ for **10** and at 1921 and 1851 cm$^{-1}$ for **11**. The molecular structures of **10** and **11** were obtained from single-crystal X-ray diffraction studies (Figure 8, Table 1). Crystals of **10** were grown from a dichloromethane solution layered with *n*-pentane. Complex **11** was crystallized from a concentrated benzene solution. Both structures show cationic complexes with triflate counterions, which were also observed by $^{19}$F{$^1$H} NMR spectroscopy (singlet at −79.6 ppm in acetone-$d_6$ for **10**; singlet at −80.1 ppm in CD$_3$CN for **11**). The rhenium(I) centers have distorted octahedral coordination spheres with a meridional chelating PNP pincer ligand. The two CO ligands bind to the metal in a mutually *cis* orientation. The axial position is occupied in both complexes by the (primary) imino ligands. The C=N bond lengths (N2–C26) are 1.288(7) Å for **10** and 1.282(3) Å for **11**, indicating the formation of C=N imino double bonds.

**Scheme 4. Reaction with MeOTf**[a]

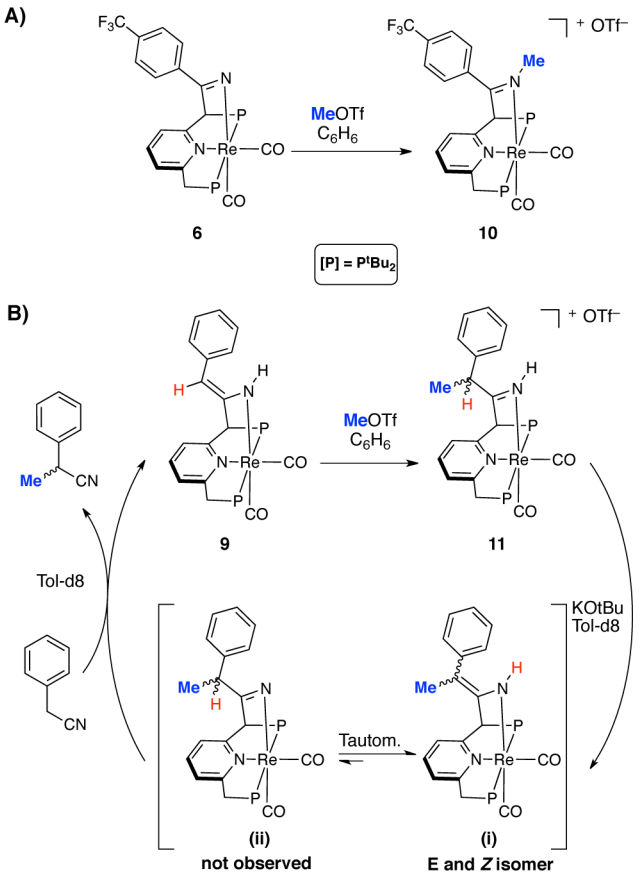


[a](A) Stoichiometric reaction of **6**. (B) A complete cycle for conversion of PhCH$_2$CN to 2-phenylpropanenitrile via complex **9**.

**Reactivity of Complex 11.** The primary imino complex **11** readily reacts with strong bases. In a NMR tube experiment, **11** was deprotonated with KO$^t$Bu in toluene-$d_8$. The resulting mixture contained two new major species with AB-spin systems in the $^{31}$P{$^1$H}NMR spectrum at 106.1 and 83.8 ppm ($^2J_{PP}$ = 189.5 Hz) and at 99.4 and 84.3 ppm ($^2J_{PP}$ = 188.7 Hz). Upon reaction with the base, the characteristic singlet resonance in the $^1$H NMR spectrum for the primary imine proton C=N*H* at 9.96 ppm disappears, indicating deprotonation of the C=N–*H* proton rather than proton abstraction from the pincer "arm". Full assignment of the two in situ formed species was challenging due to the multiple overlaps of peaks in the aliphatic and aromatic regime of the $^1$H NMR spectra. However, the smaller peak separation of the doublets in the $^{31}$P{$^1$H} NMR spectrum, as observed for complex **9**, suggests two similar enamido species.

The $^1$H NMR spectrum exhibits two sets of signals in a approximately 1:1 ratio, for methyl-, methylene-, methine-, and amido moieties, suggesting the formation of two geometrical isomers **i-*E*** and **i-*Z*** (Scheme 4B), which may result from the initial formation of ketimido complex **ii** (not observed) and subsequent tautomerization. Addition of benzyl cyanide to the mixture of **i-*E*/*Z*** furnishes the starting complex **9** with release of 2-phenylpropanenitrile, which was identified by GC–MS analysis. It is reasonable to assume that the release of 2-phenylpropanenitrile occurs via the ketimides **ii**, which is a tautomeric form of **i-*E*/*Z***. Essentially, the metal–ligand

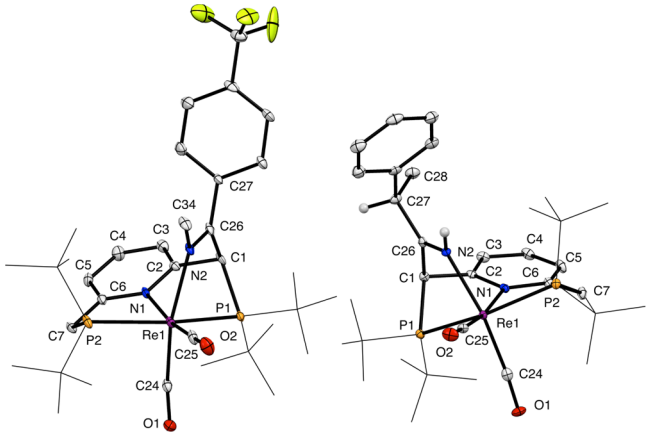


**Figure 8.** ORTEP diagram of *cis*-[Re(PNP$^{tBu}$–N(Me)=CPh$^{pCF3}$)(CO)$_2$]OTf (**10**, left) and *cis*-[Re(PNP$^{tBu}$–HN=C–CH(Me)Ph)(CO)$_2$]OTf (**11**, right) with ellipsoids at 30% probability. The P(*tert*-butyl)$_2$ groups are drawn as wire-frames. The OTf$^-$ counterions and the hydrogen atoms, except for the H of the primary imino moiety in **11**, are omitted for clarity. Selected bond lengths are given in Table 1.


dx.doi.org/10.1021/ja4071859 | J. Am. Chem. Soc. 2013, 135, 17004–17018

cooperative activation of benzyl cyanide by the dearomatized complex **4** enables a methylation−deprotonation reaction sequence, which allows for the selective monomethylation of the substrate. However, this reaction cannot be run in a one-pot reaction due to the incompatibility of MeOTf and KO$^t$Bu. Monomethylation of benzyl cyanide derivatives is an important issue in the synthesis of ibuprofen and is the subject of recent studies of environmentally benign methylations.[79,80]

**Michael Addition Triggered by MLC.** As shown above, the dearomatized complex **4** readily reacts with benzyl cyanide to form the enamido complex **9**. Both **4** and **9** were found to catalyze the Michael addition of benzyl cyanide to methyl acrylate to give methyl 4-cyano-4-phenylbutanoate (**13**, Scheme 5) with no additional base.

Benzyl cyanide and methyl acrylate (0.4 mmol scale) selectively react in THF in the presence of 2 mol% of complex **9** at 65 °C within 20 h to give **13** in 90% yield (NMR) (99% conversion of methyl acrylate). Side reactions, such as polymerization of methyl acrylate, were not observed. Stepwise addition of a second equivalent of methyl acrylate, after the reaction reached completion, resulted in a second Michael addition sequence to give dimethyl 4-cyano-4-phenylheptanedioate (**14**). The double addition product **14** was also obtained when the reaction was performed with 2.1 equiv of methyl acrylate with respect to benzyl cyanide (0.66 mmol of benzyl cyanide, 1.4 mmol of methyl acrylate, 1 mol % **9**, 80 °C oil bath temperature, 12 h, closed vessel, in THF).[81]

Other substrates can be used in the catalytic Michael addition, and the results are summarized in Table 3. Different $\alpha,\beta$-unsaturated esters and ketones were used as Michael acceptors and reacted with benzyl cyanide (entries 1−4). Likewise, as the Michael donor, other benzyl cyanide derivatives were used, including derivatives with electron-donating (entry 5) and electron-withdrawing (entry 6) substituents.

On the basis of our observations, we propose the catalytic pathway in Scheme 6. The dearomatized complex **4** binds the benzyl cyanide substrate via MLC to form the intermediate enamido complex **9** (step **I**). Subsequently, **9** is attacked by methyl acrylate to give the transient species **A** (step **II**), which rearranges to the ketimides species **B** (step **III**). A tautomeric [1,3]-H-shift gives complex **C**. The product **13** is released from **C** by Re−N and C−C bond cleavage to give the dearmomatized complex **4**, which completes the catalytic cycle (step **IV**). A similar cycle is conceivable for the Michael addition of **13** to methyl acrylate to yield **14**.

**Scheme 5. Michael Addition of Benzyl Cyanide to Methyl Acrylate Catalyzed by 4 or 9 To Selectively Give the Addition Products 13 and 14**

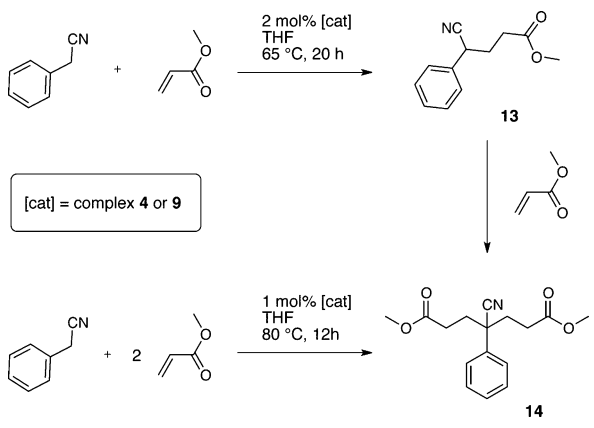


**Table 3. Catalytic Michael Additions of Benzyl Nitriles to $\alpha,\beta$-Unsaturated Esters and Ketones[a]**

| | Nitrile | Acceptor | T (°C) | Conv. (%) | Yield (%) | Product |
|---|---|---|---|---|---|---|
| 1 |  |  | 65 | >99 | 90 | 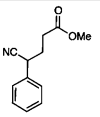 **13** |
| 2 |  |  | 65 | >99 | 55 | 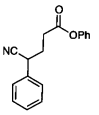 **15** |
| 3 |  |  | 25 | >99 | 73 | 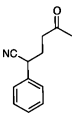 **16** |
| 4[b] |  |  | 80 | 61 | 60 | 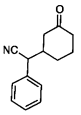 **17** |
| 5[c] |  |  | 65 | >99 | 93 | 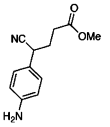 **18** |
| 6 |  |  | 80 | >99 | 90 | 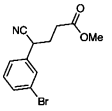 **19** |

[a]Conversion with respect to the Michael acceptor (determined by GC); yield determined by NMR; 0.4 mmol nitrile, 0.4 mmol acceptor, 2 mol% catalyst [Re(PNP$^{tBu}$−HNC═CHPh)(CO)$^2$] **9** (entries 1−4) or [Re(PNP$^{tBu}$*)(CO)$_2$] **4** (entries 5−6); reaction time 20 h. [b]Michael addition product obtained as a 1:1 mixture of diastereomers. [c]0.2 mmol nitrile and 0.2 mmol acceptor.

## SUMMARY AND CONCLUSION

We have demonstrated an unprecedented mode for activation of nitriles, based on MLC, involving reversible C−C and M−N bond formation in a rare Re(I) PNP pincer complex. Depending on the nature of the substrate, ketimido complexes are formed with nitriles lacking $\alpha$-methylene groups, and enamido complexes are formed with aliphatic nitriles. Electrophilic attack occurs at nitrogen in the ketimido complex, and selectively at the $\alpha$-carbon in the enamido complex. Our computational studies suggest a stepwise activation of the nitriles by the dearomatized complex [Re(PNP$^{tBu}$*)(CO)$_2$] (**4**) with remarkably low activation barriers, involving the precoordination of the nitrile group to the rhenium(I) center. A concerted activation, as previously found for the activation of $CO_2$ to a similar ruthenium PNP pincer complex ([Ru(PNP$^{tBu}$*)(CO)(H)]), does not occur. The novel mode of


dx.doi.org/10.1021/ja4071859 | J. Am. Chem. Soc. 2013, 135, 17004−17018

**Scheme 6. Possible Catalytic Cycle for the Michael Addition of Benzyl Cyanide to Methyl Acrylate**

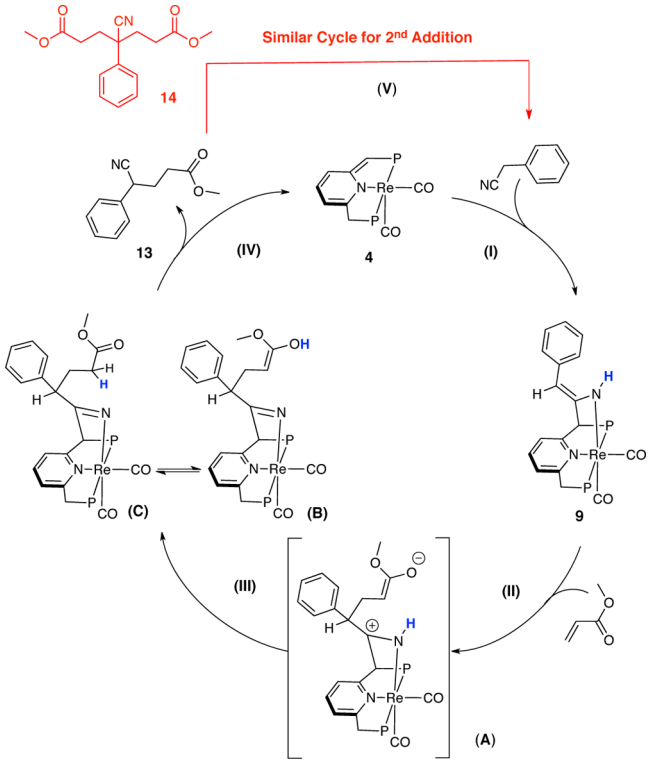


nitrile activation via MLC was utilized in reactivity studies and catalysis. A complete reaction cycle was developed for the selective monomethylation of $PhCH_2CN$ to 2-phenylpropanenitrile ($PhCH(Me)-CN$) via complex **9**. Complexes **4** and **9** are also active catalysts in Michael addition reactions with no need for added base. We are currently extending the scope of rhenium pincer-type complexes, and the activation of other unsaturated substrates with dearomatized metal complexes is a focal point of our ongoing research.

## EXPERIMENTAL SECTION

All experiments were carried out under an atmosphere of purified nitrogen in a M-BRAUN Unilab 1200/780 glovebox or using standard Schlenk techniques. All solvents were purchased "reagent grade" or better. Solvents, except methylene chloride, were refluxed over sodium/benzophenone and distilled under an argon atmosphere. Methylene chloride was used as received and dried over 4 Å molecular sieves. Deuterated solvents were used as received and degassed with argon and kept in the glovebox over 4 Å molecular sieves. The $PNP^{tBu}$ ligand was prepared according to the literature procedure.[83] Benzonitrile, propionitrile, pivalonitrile, and benzyl cyanide were distilled prior to use. $[Re(CO)_5Cl]$, KO*t*Bu, $^{pCF3}Ph-CN$, and MeOTf were used as received from Sigma-Aldrich without any further purification. NMR spectroscopy: $^1H$, $^{13}C\{^1H\}$, and $^{31}P\{^1H\}$ NMR spectra were recorded on Bruker AMX-300, AMX-400, and AMX-500 NMR spectrometers. $^1H$, $^{13}C\{^1H\}$, and $^{13}C\{^1H\}$ DEPTQ NMR chemical shifts are reported in ppm referenced to tetramethylsilane calibrated using residual solvent signals. $^{31}P\{^1H\}$ NMR chemical shifts are reported in ppm referenced to an external 85% solution of phosphoric acid in $D_2O$. Elemental analyses were performed on a Thermo Finnigan Italia S.p.A-FlashEA 1112 CHN Elemental Analyzer by the Department of Chemical Research Support, Weizmann Institute of Science. Mass spectra were recorded on MicromassPlatform LCZ 4000, using electro spray ionization (ESI) mode. GC–MS was carried out on HP 6890 (flame ionization detector and thermal conductivity detector) and HP 5973 (MS detector) instruments equipped with a 30 m column (Restek 5MS, 0.32 mm internal diameter) with a 5% phenylmethyl silicone coating (0.25 mm) and helium as carrier gas. GC analysis were carried out using a Carboxen 1000 column on a HP 690 series GC system or HP-5 cross-linked 5% phenylmethylsilicone column (30 m × 0.32 mm × 0.25 $\mu$m film thickness, FID) on a HP 6890 series GC system using 1,3,5-tris-isopropyl benzene or mesitylen as an internal standard. Crystallographic details are as follows. For complex **3**, crystal data: $C_{25}H_{43}ClNO_2P_2Re$, orange plate, 0.33 × 0.33 × 0.12 mm$^3$, monoclinic $P2(1)/c$, $a$ = 14.6158(2) Å, $b$ = 12.1609(2) Å, $c$ = 16.1492(2) Å, $\beta$ = 101.0602(10)° from 8178 reflections, $T$ = 120(2) K, $V$ = 2817.05(7) Å$^3$, $Z$ = 4, $F_w$ = 673.19, $D_c$ = 1.587 Mg m$^{-3}$, $\mu$ = 4.543 mm$^{-1}$. Data collection and processing: Nonius KappaCCD diffractometer, Mo K$\alpha$ ($\lambda$ = 0.71073 Å), graphite monochromator, MiraCol optics, $-20 \le h \le 20$, $-17 \le k \le 17$, $-22 \le l \le 22$, frame scan width = 1.0°, scan speed 1.0° per 15 s, typical peak mosaicity 0.46°, 42 412 reflections collected, 8571 independent reflections ($R$-int = 0.039). The data were processed with DenzoHKL-Scalepack. Solution and refinement: Structure solved with SHELXS. Full matrix least-squares refinement based on $F^2$ with SHELXL-97 on 295 parameters with no restraints gave final R1 = 0.0316 (based on $F^2$) for data with $I > 2\sigma(I)$ and R1 = 0.0398 on 8216 reflections, Goof on $F^2$ = 1.036, largest electron density peak 4.039 e Å$^{-3}$. Largest hole −2.152 e Å$^{-3}$. For complex **4**, crystal data: $C_{25}H_{42}NO_2P_2Re$, green/black prism, 0.28 × 0.20 × 0.17 mm$^3$, orthorhombic *Pnaa*, $a$ = 11.3342(1) Å, $b$ = 15.5145(3) Å, $c$ = 30.5847(4) Å from 57 207 reflections, $T$ = 120(2) K, $V$ = 5378.2(2) Å$^3$, $Z$ = 8, $F_w$ = 636.74, $D_c$ = 1.573 Mg m$^{-3}$, $\mu$ = 4.659 mm$^{-1}$. Data collection and processing: Nonius KappaCCD diffractometer, Mo K$\alpha$ ($\lambda$ = 0.71073 Å), graphite monochromator, MiraCol optics, $0 \le h \le 13$, $0 \le k \le 18$, $0 \le l \le 36$, frame scan width = 0.5°, scan speed 1.0° per 20 s, typical peak mosaicity 0.58°, 24 275 reflections collected, 6742 independent reflections ($R$-int = 0.091). The data were processed with Denzo HKL2000. Solution and refinement: Structure solved with SHELXS. Full matrix least-squares refinement based on $F^2$ with SHELXL-97 on 292 parameters with 0 restraints gave final R1 = 0.0587 (based on $F^2$) for data with $I > 2\sigma(I)$ and R1 = 0.0793 on 4870 reflections, Goof on $F^2$ = 1.065, largest electron density peak 4.293 e Å$^{-3}$. Largest hole −1.429 e Å$^{-3}$. For complex **5**, crystal data: $C_{32}H_{47}N_2O_2P_2Re$, orange plate, 0.40 × 0.19 × 0.09 mm$^3$, monoclinic $P2(1)/c$, $a$ = 8.9108(1)Å, $b$ = 18.0558(4)Å, $c$ = 20.9380(4)Å, $\beta$ = 106.4490(14)° from 48 538 reflections, $T$ = 120(2) K, $V$ = 3230.87(10) Å$^3$, $Z$ = 4, $F_w$ = 739.86, $D_c$ = 1.5251 Mg m$^{-3}$, $\mu$ = 3.890 mm$^{-1}$. Data collection and processing: Nonius KappaCCD diffractometer, Mo K$\alpha$ ($\lambda$ = 0.71073 Å), graphite monochromator, MiraCol optics, $-11 \le h \le 11$, $-22 \le k \le 23$, $-27 \le l \le 26$, frame scan width = 1.0°, scan speed 1.0° per 60 s, typical peak mosaicity 0.63°, 31 074 reflections collected, 7359 independent reflections ($R$-int = 0.0646). The data were processed with Denzo HKL2000. Solution and refinement: Structure solved with SHELXS. Full matrix least-squares refinement based on $F^2$ with SHELXL-97 on 364 parameters with 0 restraints gave final R1 = 0.0434 (based on $F^2$) for data with $I > 2\sigma(I)$ and R1 = 0.0663 on 7359 reflections, Goof on $F^2$ = 1.041, largest electron density peak 1.764 e Å$^{-3}$. Largest hole −1.425 e Å$^{-3}$. For complex **7**, crystal data: $C_{30}H_{51}N_2O_2P_2Re + C_5H_9N$, orange prism, 0.20 × 0.20 × 0.10 mm$^3$, monoclinic $P2(1)/n$, $a$ = 12.4882(2) Å, $b$ = 22.7280(4) Å, $c$ = 13.5870(2) Å, $\beta$ = 104.861(1)° from 35 290 reflections, $T$ = 120(2) K, $V$ = 3725.79(11) Å$^3$, $Z$ = 4, $F_w$ = 803.00, $D_c$ = 1.432 Mg m$^{-3}$, $\mu$ = 3.380 mm$^{-1}$. Data collection and processing: Nonius KappaCCD diffractometer, Mo K$\alpha$ ($\lambda$ = 0.71073 Å), graphite monochromator, MiraCol optics, $17 \le h \le 17$, $-32 \le k \le 29$, $-19 \le l \le 19$, frame scan width = 1.0°, scan speed 1.0° per 20 s, typical peak mosaicity 0.45°, 35 789 reflections collected, 11 162 independent reflections ($R$-int = 0.088). The data were processed with Denzo HKL2000. Solution and refinement: Structure solved with SHELXS. Full matrix least-squares refinement based on $F^2$ with SHELXL-97 on 376 parameters with 0 restraints gave final $R_1$ = 0.0479 (based on $F^2$) for data with $I > 2\sigma(I)$ and $R_1$ = 0.0749 on 10 895 reflections, Goof on $F^2$ = 1.125, largest electron density peak 5.260 e Å$^{-3}$. Largest hole −1.739 e Å$^{-3}$. For complex **8**, crystal data: $(2*(C_{28}H_{47}N_2O_2P_2Re_1) + C_5H_{12})$ orange plate, 0.09 × 0.08 × 0.03 mm$^3$, monoclinic, $P2(1)/c$, $a$


dx.doi.org/10.1021/ja4071859 | J. Am. Chem. Soc. 2013, 135, 17004–17018

= 13.118(3), $b$ = 14.918(3), $c$ = 16.915(3) Å, $\beta$ = 99.27(3)° from 20° of data, $T$ = 120(2) K, $V$ = 3266.9(11) Å$^3$, $Z$ = 2, $F_w$ = 1455.78, $D_c$ = 1.480 Mg m$^{-3}$, $\mu$ = 3.846 mm$^{-1}$. Data collection and processing: Nonius KappaCCD diffractometer, Mo K$\alpha$ ($\lambda$ = 0.71073 Å), graphite monochromator, 13 983 reflections collected, $-16 \le h \le 16$, $0 \le k \le 19$, $0 \le l \le 21$, frame scan width = 0.5°, scan speed 1.0° per 180 s, typical peak mosaicity 0.69°, 7182 independent reflections ($R$-int = 0.0372). The data were processed with Denzo-Scalepack. Solution and refinement: Structure solved by direct methods with SHELXS-97. Full matrix least-squares refinement based on $F^2$ with SHELXL-97. 382 parameters with 0 restraints, final $R_1$ = 0.0389 (based on $F^2$) for data with $I > 2\sigma(I)$ and $R_1$ = 0.0623 on 7182 reflections, Goof on $F^2$ = 1.026, largest electron density peak = 4.477 e Å$^{-3}$, deepest hole −1.677 e Å$^{-3}$. For complex **9**, crystal data: ($C_{33}H_{49}N_2O_2P_2Re_1$ + $C_6H_6$), yellow prism, 0.12 × 0.12 × 0.08 mm$^3$, triclinic, $P\bar{1}$, $a$ = 12.124(2), $b$ = 13.337(3), $c$ = 13.581(3) Å, $\alpha$ = 113.99(3)°, $\beta$ = 91.15(3)°, $\gamma$ = 106.97(2)° from 20° of data, $T$ = 120(2) K, $V$ = 1894.6(9) Å$^3$, $Z$ = 2, $F_w$ = 831.99, $D_c$ = 1.458 Mg m$^{-3}$, $\mu$ = 3.326 mm$^{-1}$. Data collection and processing: Nonius KappaCCD diffractometer, Mo K$\alpha$ ($\lambda$ = 0.71073 Å), graphite monochromator, 17 055 reflections collected, $-15 \le h \le 15$, $-17 \le k \le 16$, $0 \le l \le 17$, frame scan width = 1°, scan speed 1.0° per 60 s, typical peak mosaicity 0.48°, 9007 independent reflections ($R$-int = 0.0242). The data were processed with Denzo-Scalepack. Solution and refinement: Structure solved by direct methods with SHELXS-97. Full matrix least-squares refinement based on $F^2$ with SHELXL-97. 439 parameters with 1 restraints, final $R_1$ = 0.0281 (based on $F^2$) for data with $I > 2\sigma(I)$ and $R_1$ = 0.0350 on 9007 reflections, Goof on $F^2$ = 1.100, largest electron density peak = 3.068 e Å$^{-3}$, deepest hole −1.199 e Å$^{-3}$. For complex **10**, crystal data: $C_{34}H_{49}F_3N_2O_2P_2Re$ + $CF_3O_3S$ + $CH_2Cl_2$, yellow plate, 0.40 × 0.30 × 0.20 mm$^3$, monoclinic $P2(1)/c$, $a$ = 12.7580(1) Å, $b$ = 9.2810(1) Å, $c$ = 35.6750(4) Å, $\beta$ = 94.6930(4)° from 41 887 reflections, $T$ = 120(2) K, $V$ = 4210.01(7) Å$^3$, $Z$ = 4, $F_w$ = 1056.89, $D_c$ = 1.667 Mg m$^{-3}$, $\mu$ = 3.208 mm$^{-1}$. Data collection and processing: Nonius KappaCCD diffractometer, Mo K$\alpha$ ($\lambda$ = 0.71073 Å), graphite monochromator, MiraCol optics, $-15 \le h \le 15$, $-8 \le k \le 11$, $-42 \le l \le 42$, frame scan width = 0.5°, scan speed 1.0° per 14 s, typical peak mosaicity 0.36°, 41 887 reflections collected, 17 455 independent reflections ($R$-int = 0.112). The data were processed with Denzo HKL2000. Solution and refinement: Structure solved with SHELXS. Full matrix least-squares refinement based on $F^2$ with SHELXL-97 on 364 parameters with 0 restraints gave final $R_1$ = 0.0477 (based on $F^2$) for data with $I > 2\sigma(I)$ and $R_1$ = 0.0574 on 7681 reflections, Goof on $F^2$ = 1.097, largest electron density peak 5.936 e Å$^{-3}$. Largest hole −2.680 e Å$^{-3}$. For complex **11**, crystal data: ($C_{34}H_{52}N_2O_2P_2Re_1$ + $C_1F_3O_3S_1$ + 1.5*$C_6H_6$) yellow plate, 0.15 × 0.08 × 0.02 mm$^3$, triclinic, $P\bar{1}$, $a$ = 9.637(2), $b$ = 12.321(3), $c$ = 19.322(4) Å, $\alpha$ = 88.76(3)°, $\beta$ = 80.82(2)°, $\gamma$ = 85.69(3)° from 20° of data, $T$ = 100(2) K, $V$ = 2258.3(8) Å$^3$, $Z$ = 2, $F_w$ = 1035.15, $D_c$ = 1.522 Mg m$^{-3}$, $\mu$ = 2.865 mm$^{-1}$. Data collection and processing: Bruker Apex2 KappaCCD diffractometer, Mo K$\alpha$ ($\lambda$ = 0.71073 Å), graphite monochromator, 55 196 reflections collected, $-12 \le h \le 12$, $-15 \le k \le 15$, $-25 \le l \le 25$, frame scan width = 0.5°, scan speed 1.0° per 40 s, typical peak mosaicity 0.83°, 10 274 independent reflections ($R$-int = 0.0456). The data were processed with Bruker Apex2. Solution and refinement: Structure solved by direct methods with SHELXS-97. Full matrix least-squares refinement based on $F^2$ with SHELXL-97. 540 parameters with 0 restraints, final $R_1$ = 0.0234 (based on $F^2$) for data with $I > 2\sigma(I)$ and $R_1$ = 0.0287 on 10 274 reflections, Goof on $F^2$ = 1.027, largest electron density peak = 1.012 e Å$^{-3}$, deepest hole −0.956 e Å$^{-3}$.

**Computational Methods.** All calculations were performed using Gaussian 09 Revision C.01.[84] Two density functional theory (DFT) exchange-correlation functionals were used. Geometries were optimized and vibrational frequencies were calculated using the Perdew–Burke–Ernzerhof (PBE) generalized-gradient approximation (GGA) functional.[85,86] Accurate energies were calculated using one of the latest double-hybrid functionals by Kozuch and Martin: DSD-PBEP86.[87] This double-hybrid functional incorporates the Perdew–Burke–Ernzerhof (PBE),[85,86,88] DFT exchange functional with "exact" Hartree–Fock exchange, the Perdew-86 correlation functional[89] with spin-component scaled,[90,91] second-order Møller–Plesset[92] (SCS-MP2)-like correlation, and an empirical dispersion correction,[93−96] specifically Grimme's third version of his empirical dispersion correction (DFTD3)[93,97] with Becke–Johnson (BJ) dampening.[97,98] Two basis set-RECP (relativistic effective core potential) combinations were used. The first, denoted SDD(d), is the combination of the Huzinaga–Dunning double-$\zeta$ basis set[99] on lighter elements with the Stuttgart–Dresden basis set-RECP combination[100] on transition metals; polarization functions (i.e., the D95(d) basis set) were added to second-row (i.e., phosphorus) atoms. The second is denoted as cc-pV(D+d)Z-PP, which includes the Dunning cc-pVDZ basis set[101] on H, C, N, and O, Wilson's cc-pV(D+d) on P,[102] and Peterson's cc-pVDZ-PP basis set-RECP on Ru.[103] Geometry optimizations and frequency calculations were carried out using the former basis set, while the energetics of the reaction were calculated at these geometries with the latter basis set. When using the PBE functional, density fitting basis sets, specifically the fitting sets generated using the automatic generation algorithm implemented in Gaussian 09, were used to speed up the calculations.[104,105] The accuracy of the DFT method was improved by adding the empirical dispersion correction as recommended by Grimme.[93,95] The older version (DFTD2)[95] is available, with analytical gradients and Hessians, in Gaussian 09 and was used during geometry optimizations and frequency calculations; our version of Gaussian 09 was locally modified to allow for its use for any DFT functional rather than just the limited set included in the commercially available version. As noted above, DSD-PBEP86 includes, per definition, a DFTD3 correction with BJ-scaling in its functional form, which was calculated using a program written by Grimme.[93] Bulk solvent effects were approximated by single point energy calculations using a polarizable continuum model (PCM),[106−109] specifically the integral equation formalism model (IEF-PCM)[106,107,110,111] with $n$-pentane as the solvent as in the experiments. Specifically, Truhlar's empirically parametrized version Solvation Model Density (SMD) was used.[112] Geometries were optimized using the default pruned (75,302) grid, while the "ultrafine" (i.e., a pruned (99,590)) grid was used for energy and solvation calculations.

***cis*-[Re(PNP$^{t\mathrm{Bu}}$)(CO)$_2$Cl] (3).** A solution of 2,6-bis(di-$^t$butylphosphinomethyl)pyridine) (870 mg, 2.20 mmol) in 4 mL of THF was added to a stirred suspension of [Re(CO)$_5$Cl] (800 mg, 2.20 mmol) in 4 mL of THF. The reaction mixture was transferred to a pressure tube and heated at 80 °C overnight in the closed vessel. The obtained yellow solution was then concentrated by partial evaporation of the solvent in vacuo. The product **3** was crystallized by layering the THF solution with $n$-pentane. The crystals were decanted, washed with $n$-pentane, and dried in vacuo. Yield: 1037 mg, 70%. $^1$H NMR (400.36 MHz, $CD_2Cl_2$, 25 °C) $\partial$: 1.33 (t, $^3J_{PH}$ = 6.30 Hz, 18H, ((C$H_3$)$_3$CP), 1.38 (t, $^3J_{PH}$ = 6.30 Hz, 18H, ((C$H_3$)$_3$CP), 3.61 (d, $^2J_{HH}$ = 15.70 Hz, 2H, PC$H_2$), 4.22 (d, $^2J_{HH}$ = 15.70 Hz, 2H, PC$H_2$), 7.36 (d, $^3J_{HH}$ = 7.8 Hz, 2H, C$H_{pyri(3,5)}$), 7.62 (t, $^3J_{HH}$ = 7.80 Hz, 1H, C$H_{pyri(4)}$) ppm. $^{31}$P{$^1$H} NMR (121.5 MHz, tol-$d_8$, 25 °C) $\partial$: 68.8 (s, 2P) ppm. $^{13}$C{$^1$H} QDEPT NMR (100.7 MHz, $CD_2Cl_2$, 25 °C) $\partial$: 32.1 (s, 3C, (C$H_3$)$_3$CP), 32.9 (s, 3C, (C$H_3$)$_3$CP), 40.3 (m, 2C, (C$H_3$)$_3$CP)), 41.5 (t, $^1J_{PC}$ = 7.2 Hz, 2C, PC$H_2$), 122.6 (t, $^3J_{PC}$ = 4.0 Hz, 2C, C$H_{pyri(3,5)}$), 139.7 (s, 1C, C$H_{pyri(4)}$), 166.9 (t, $^2J_{PC}$ = 3.5 Hz, 2C, C$_{pyri(2,6)}$), 203.7 (m, 1C, Re−CO), 210.6 (m, 1C, Re−CO) ppm. IR (KBr, pellet) $\nu$ [cm$^{-1}$]: 1816, 1900 (1:1 ratio). Anal. Calcd for $C_{25}H_{43}ClNO_2P_2Re$: C, 44.60; H, 6.44; N, 2.08. Found: C, 44.66; H, 6.35; N, 1.93.

**[Re(PNP$^{t\mathrm{Bu}}$*)(CO)$_2$] (4).** Complex **3** (200 mg, 0.30 mmol) was dissolved in 4 mL of THF, and the yellow solution was cooled to −38 °C in the freezer. KO$^t$Bu (33 mg, 0.30 mmol) dissolved in 2 mL of THF was added dropwise to the precooled solution. The deep green solution was allowed to stir for 0.5 h at ambient temperature. Subsequently, all volatiles were evaporated in vacuo, and the remaining green solid was extracted with $n$-pentane (~30 mL) and filtered through a syringe filter (Teflon, 0.2 $\mu$m pore size). Large green crystals formed upon concentration of the filtrate. The volume of the solution was eventually reduced to ~10 mL, via partial evaporation of the solvent in vacuo, and allowed to finish the crystallization at −38 °C in the freezer for 24 h. The crystals were decanted and dried in vacuo.

Yield: 191 mg, 85%. $^1$H NMR (500.13 MHz, toluene-$d_8$, 25 °C) $\partial$: 1.03 (d, $^3J_{PH}$ = 13.30 Hz, 18H, ((C$H_3$)$_3$CP), 1.32 (d, $^3J_{PH}$ = 13.30 Hz, 18H, ((C$H_3$)$_3$CP), 2.74 (d, $^2J_{HP}$ = 9.20 Hz, 2H, PC$H_2$), 4.06 (s, 1H, PC$H$), 5.29 (d, $^3J_{HH}$ = 6.20 Hz, 1H, C$H_{pyri(3)}$), 6.17 (m, 1H, C$H_{pyri(4)}$), 6.27 (d, $^3J_{HH}$ = 9.00 Hz, 1H, C$H_{pyri(5)}$) ppm. $^{31}$P{$^1$H} NMR (121.5 MHz, toluene-$d_8$, 25 °C) $\partial$: 68.9 (d, $^2J_{PP}$ = 145.0 Hz, 1P, $P$CH=C), 74.7 (d, $^2J_{PP}$ = 145.0 Hz, 1P, $P$CH$_2$C)) ppm. $^{13}$C{$^1$H} QDEPT NMR (100.7 MHz, $CD_2Cl_2$, 25 °C) $\partial$: 29.6 (d, $^2J_{CP}$ = 4.5 Hz, 3C, (C$H_3$)$_3$CP), 30.0 (d, $^2J_{CP}$ = 3.9 Hz, 3C, (C$H_3$)$_3$CP), 36.2 (d, $^1J_{CP}$ = 18.7 Hz, 1C, PC$H_2$), 37.6 (d, $^1J_{CP}$ = 19.6 Hz, 1C, (CH$_3$)$_3$$C$P), 38.1 (d, $^1J_{CP}$ = 26.2 Hz, 1C, (CH$_3$)$_3$$C$P), 76.3 (d, $^1J_{CP}$ = 50.3 Hz, 1C, PCH=C), 99.7 (d, $^3J_{PC}$ = 10.2 Hz, 1C, C$H_{pyri(3)}$), 118.4 (d, $^3J_{PC}$ = 16.6 Hz, 1C, C$H_{pyri(5)}$), 131.6 (s, 1C, C$H_{pyri(4)}$), 161.8 (t, $^2J_{CP}$ = 5.8 Hz, 1C, $C_{pyri(6)}$), 175.1 (dd, $^{2,3}J_{PC}$ = 5.2 Hz, 17.4 Hz, 1C, $C_{pyri(2)}$), 208.4 (t, $^2J_{CP}$ = 5.1 Hz, 2C, Re−CO) ppm. IR (KBr, pellet) $\nu$ [cm$^{-1}$]: 1826, 1905 ($\nu_{CO}$, 1:1 ratio). Anal. Calcd for $C_{25}H_{42}NO_2P_2Re$: C, 47.16; H, 6.65; N, 2.20. Found: C, 47.19; H, 6.94; N, 1.95.

***cis*-[Re(PNP$^{tBu}$−N=CPh)(CO)$_2$] (5).** KO$t$Bu (25 mg, 0.22 mmol, 1 equiv) was added to a stirred solution of **3** (150 mg, 0.22 mmol) in 3 mL of THF. After 1 h, all volatiles were evaporated in vacuo, and the residue was extracted in $n$-pentane (2 × 15 mL) and filtered through a syringe filter (Teflon, 0.2 $\mu$m pore size). The filtrate was split into two 20 mL vials, and subsequently to each vial two drops of benzonitrile (excess) were added. Orange crystals separated from the orange-red solution at −38 °C in the freezer within 48 h. The product was decanted, washed with $n$-pentane, and dried in vacuo. For a second and third crystallization, the mother liquor was each time concentrated and allowed to crystallize at −38 °C. The obtained second and third fractions were treated likewise. Yield of the combined fractions: 135 mg, 82%. $^1$H NMR (500.13 MHz, $C_6D_6$ 25 °C) $\partial$: 0.78 (s, br, 9H, (C$H_3$)$_3$CP), 1.09 (d, $^3J_{PH}$ = 11.50 Hz, 9H, (C$H_3$)$_3$CP), 1.32 (d, $^3J_{PH}$ = 12.50 Hz, 9H, (C$H_3$)$_3$CP), 1.54 (d, $^3J_{PH}$ = 13.00 Hz, 9H, (C$H_3$)$_3$CP), 3.15 (dd, $^2J_{HH}$ = 15.50 Hz, $^2J_{HP}$ = 5.00 Hz, 1H, PC$H_2$), 3.22 (dd, $^2J_{HH}$ = 15.50 Hz, $^2J_{HP}$ = 9.10 Hz, 1H, PC$H_2$), 6.19 (dd, $^2J_{HP}$ = 6.50 Hz, $^4J_{HP}$ = 1.00 Hz, 1H, PC$H$), 6.27 (d, $^3J_{HH}$ = 7.00 Hz, 1H, C$H_{py}$), 6.68 (d, $^3J_{HH}$ = 7.50 Hz, 1H, C$H_{py}$), 6.74 (t, $^3J_{HH}$ = 7.50 Hz, 1H, C$H_{py(5)}$), 7.12 (t, $^3J_{HH}$ = 7.50 Hz, 1H, C$H_{Ar}$), 7.27 (t, $^3J_{HH}$ = 7.50 Hz, 2H, C$H_{Ar}$), 8.05 (d, $^3J_{HH}$ = 8.00 Hz, 2H, C$H_{Ar}$) ppm. $^{31}$P{$^1$H} NMR (202.5 MHz, $C_6D_6$, 25 °C) $\partial$: 86.7 (d, $^2J_{PP}$ = 193.8 Hz, 1P), 128.2 (d, $^2J_{PP}$ = 193.8 Hz, 1P) ppm. $^{13}$C{$^1$H} QDEPT NMR (125.8 MHz, $C_6D_6$, 25 °C) $\partial$: 29.8 (s, br, 3C, (CH$_3$)$_3$CP), 30.2 (s, br, 3C, (CH$_3$)$_3$CP), 30.9 (d, 3C, $^2J_{CP}$ = 3.8 Hz, (CH$_3$)$_3$CP), 32.1 (d, 3C, $^2J_{CP}$ = 3.3 Hz, (CH$_3$)$_3$CP), 36.1 (d, $^1J_{CP}$ = 7.5 Hz, 1C, (CH$_3$)$_3$CP), 37.7 (d, $^1J_{CP}$ = 10.6 Hz, 1C, (CH$_3$)$_3$CP), 38.0 (t, $J_{CP}$ = 7.0 Hz, 1C, (CH$_3$)$_3$CP), 38.5 (d, $^1J_{CP}$ = 20.8 Hz, 1C, (CH$_3$)$_3$CP), 40.1 (d, $^1J_{CP}$ = 17.0 Hz, 1C, PCH$_2$), 66.0 (d, $^1J_{CP}$ = 23.0 Hz, 1C, PCH=CN), 116.6 (d, $^3J_{PC}$ = 6.7 Hz, 1C, C$H_{py}$), 117.8 (d, $^3J_{PC}$ = 6.7 Hz, 1C, C$H_{py}$), 126.8 (s, 2C, C$H_{Ar}$), 128.3 (s, 1C, C$H_{Ar}$), 128.6 (s, 2C, C$H_{Ar}$), 135.6 (s, 1C, C$H_{py}$), 139.5 (s, 1C, $C_{Ar}$), 154.8 (dd, $^2J_{PC}$ = 16.5 Hz, $^3J_{PC}$ = 4.5 Hz, 1C, C=N), 161.4 (t, br, $^2J_{PC}$ = 6.5 Hz, 1C, $C_{py}$), 164.0 (d, $^2J_{PC}$ = 1.6 Hz, 1C, $C_{py}$), 211.0 (t, $^2J_{CP}$ = 5.4 Hz, 1C, Re−CO), 215.4 (t, $^2J_{CP}$ = 5.5 Hz, 1C, Re−CO) ppm. IR (KBr, pellet) $\nu$ [cm$^{-1}$]: 1816, 1888 ($\nu_{CO}$, 1:1 ratio). Anal. Calcd for $C_{32}H_{47}N_2O_2P_2Re$: C, 51.95; H, 6.40; N, 3.79. Found: C, 52.29; H, 6.30; N, 3.47. MS (ESI-TOF) found M$^+$ = 638.23 (**5** − PhCN) + H$^+$.

***cis*-[Re(PNP$^{tBu}$−N=CPh$^{pCF3}$)(CO)$_2$] (6).** KO$t$Bu (10 mg, 0.09 mmol, 1 equiv) was added to a stirred solution of **3** (62 mg, 0.09 mmol) in 3 mL of THF in a 20 mL vial. After 20 min, all volatiles were evaporated in vacuo, and the residue was extracted in $n$-pentane (15 mL) and filtered through a syringe filter (Teflon, 0.2 $\mu$m pore size). Subsequently, 4-(trifluoromethyl)benzonitrile (24 mg, 0.14 mmol, 1.5 equiv) was added to the stirred solution, and an immediate color change to orange occurred. Orange-brown crystalline flakes precipitated upon stirring for further 15 min at ambient temperature. The product was decanted from the almost colorless supernatant solution, washed with $n$-pentane (10 mL), and dried in vacuo. Yield: 62 mg, 83%. $^1$H NMR (500.13 MHz, $C_6D_6$, 25 °C) $\partial$: 0.73 (s, br, 9H, (C$H_3$)$_3$CP), 1.07 (d, $^3J_{PH}$ = 11.50 Hz, 9H, (C$H_3$)$_3$CP), 1.26 (d, $^3J_{PH}$ = 12.50 Hz, 9H, (C$H_3$)$_3$CP), 1.54 (d, $^3J_{PH}$ = 13.00 Hz, 9H, (C$H_3$)$_3$CP), 2.98 (dd, $^2J_{HH}$ = 15.50 Hz, $^2J_{HP}$ = 5.00 Hz, 1H, PC$H_2$), 3.21 (dd, $^2J_{HH}$ = 15.50 Hz, $^2J_{HP}$ = 9.00 Hz, 1H, PC$H_2$), 6.04 (d, $^2J_{HP}$ = 6.50 Hz, 1H, PC$H$), 6.29 (d, $^3J_{HH}$ = 7.50 Hz, 1H, C$H_{py}$), 6.64 (d, $^3J_{HH}$ = 7.50 Hz, 1H, C$H_{py}$), 6.81 (t, $^3J_{HH}$ = 7.50 Hz, 1H, C$H_{py(4)}$), 7.49 (d, $^3J_{HH}$ = 8.50 Hz, 2H, C$H_{Ar}$), 7.91 (d, $^3J_{HH}$ = 8.00 Hz, 2H, C$H_{Ar}$) ppm. $^{31}$P{$^1$H} NMR (202.5 MHz, $C_6D_6$, 25 °C) $\partial$: 86.6 (d, $^2J_{PP}$ = 192.2 Hz, 1P), 129.4 (d, $^2J_{PP}$ = 191.7 Hz, 1P) ppm. $^{13}$C{$^1$H} QDEPT NMR (125.8 MHz, $C_6D_6$, 25 °C) $\partial$: 29.7 (d, br, $^2J_{CP}$ = 3.5 Hz, 3C, (CH$_3$)$_3$CP), 30.1 (d, br, $^2J_{CP}$ = 1.8 Hz, 3C, (CH$_3$)$_3$CP), 30.9 (d, 3C, $^2J_{CP}$ = 3.4 Hz, (C$H_3$)$_3$CP), 32.1 (d, 3C, $^2J_{CP}$ = 3.6 Hz, (C$H_3$)$_3$CP), 36.1 (d, $^1J_{CP}$ = 7.4 Hz, 1C, (CH$_3$)$_3$CP), 37.7 (dd, $^1J_{CP}$ = 10.6 Hz, $^3J_{CP}$ = 1.5 Hz, 1C, (CH$_3$)$_3$CP), 38.0 (dd, $J_{CP}$ = 6.2 Hz, $J_{CP}$ = 6.0 Hz, 1C, (CH$_3$)$_3$CP), 38.5 (d, $^1J_{CP}$ = 21.0 Hz, 1C, (CH$_3$)$_3$CP), 40.1 (d, $^1J_{CP}$ = 16.9 Hz, 1C, PCH$_2$), 65.8 (d, $^1J_{CP}$ = 22.1 Hz, 1C, PCH=CN), 116.9 (d, $^3J_{PC}$ = 6.8 Hz, 1C, C$H_{py}$), 117.8 (d, $^3J_{PC}$ = 6.5 Hz, 1C, C$H_{py}$), 125.3 (q (partially obscured), $^1J_{FC}$ = 271.7 Hz, 1C, $CF_3$), 125.7 (q, br, $^3J_{FC}$ = 3.8 Hz, 2C, C$H_{Ar}$), 126.8 (s, 2C, C$H_{Ar}$), 129.3 (d, $^2J_{FC}$ = 32.0 Hz 1C, $C_{Ar}$), 135.8 (s, 1C, C$H_{py}$), 141.5 (s, 1C, $C_{Ar}$), 154.4 (dd, $^2J_{PC}$ = 16.4 Hz, $^3J_{PC}$ = 4.8 Hz, 1C, C=N), 161.0 (dd, $^2J_{PC}$ = 5.0 Hz, $^3J_{PC}$ = 4.8 Hz, 1C, $C_{py}$), 164.2 (m, br, 1C, $C_{py}$), 210.8 (t, $^2J_{CP}$ = 5.0 Hz, 1C, Re−CO), 215.4 (t, $^2J_{CP}$ = 6.54 Hz, 1C, Re−CO) ppm. $^{19}$F{$^1$H} NMR (282.4 MHz, $C_6D_6$, 25 °C) $\partial$: 62.6 (s, 3F, $CF_3$) ppm. IR (KBr, pellet) $\nu$ [cm$^{-1}$]: 1807, 1894 ($\nu_{CO}$, 1:1 ratio). Anal. Calcd for $C_{33}H_{46}F_3N_2O_2P_2Re$: C, 49.06; H, 5.74; N, 3.4. Found: C, 49.73; H, 5.84; N, 3.23. MS (ESI-TOF) found M$^+$ = 809.26 (**6** + H$^+$).

***cis*-[Re(PNP$^{tBu}$−N=C$^t$Bu)(CO)$_2$] (7).** KO$t$Bu (10 mg, 0.09 mmol, 1 equiv) was added to a stirred solution of **3** (62 mg, 0.09 mmol) in 3 mL of THF in a 20 mL vial. After 20 min, all volatiles were evaporated in vacuo, and the residue was extracted with $n$-pentane (15 mL) and filtered through a syringe filter (Teflon, 0.2 $\mu$m pore size). Subsequently, a large excess of pivalonitrile (1 mL) was added to the stirred solution, and a color change to brown was observed. A bright red solution was observed at low temperature. The mixture was allowed to crystallize for 24 h at −38 °C. The obtained red crystals (suitable for X-ray diffraction analysis, $^t$BuCN cocrystallizes in lattice) were decanted from the almost colorless supernatant solution, washed with cold $n$-pentane, and dried in vacuo. Yield: 65 mg, 98%. Note: In some cases, colorless crystals of excess $^t$BuCN are formed in the cold, which are quickly dissolving upon warming to room temperature. $^1$H NMR (500.13 MHz, toluene-$d_8$, −65 °C) $\partial$: −0.38 (d, br, 3H, $^3J_{PH}$ = 10.00 Hz (C$H_3$)$_3$CP), 0.73 (s, 9H, (C$H_3$)$_3$C), 0.92 (s, br, 3H, (C$H_3$)$_3$CP), 1.19 (s, br, 9H, (C$H_3$)$_3$CP), 1.44 (d, $^3J_{PH}$ = 11.50 Hz, 9H, (C$H_3$)$_3$CP), 1.54 (d, $^3J_{PH}$ = 12.00 Hz, 9H, (C$H_3$)$_3$CP), 1.95 (d, $^3J_{PH}$ = 17.00 Hz, 3H, (C$H_3$)$_3$CP), 2.77 (d, br, $^2J_{HH}$ = 17.00 Hz, 1H, PC$H_2$), 3.07 (dd, $^2J_{HH}$ = 15.50 Hz, $^2J_{HP}$ = 8.50 Hz, 1H, PC$H_2$), 5.55 (d, $^2J_{HP}$ = 5.50 Hz, 1H, PC$H$), 6.31 (d, $^3J_{HH}$ = 7.50 Hz, 1H, C$H_{py}$), 6.38 (d, $^3J_{HH}$ = 7.00 Hz, 1H, C$H_{py}$), 6.88 (t, $^3J_{HH}$ = 7.50 Hz, 1H, C$H_{py(4)}$) ppm. $^{31}$P{$^1$H} NMR (202.5 MHz, toluene-$d_8$, −65 °C) $\partial$: 85.9 (d, $^2J_{PP}$ = 195.3 Hz, 1P, $P$CH$_2$), 132.3 (d, $^2J_{PP}$ = 195.3 Hz, 1P, $P$CH(N=C)) ppm. $^{13}$C{$^1$H} QDEPT NMR (125.8 MHz, toluene-$d_8$, −65 °C) $\partial$: 27.6 (s, 3C, (CH$_3$)$_3$C), 27.1 (s, br, 1C, (CH$_3$)$_3$CP), 29.6 (s, br, partly obscured, 3C, (CH$_3$)$_3$CP), 29.7 (s, br, 3C, (CH$_3$)$_3$CP), 30.3 (s, br, 1C, (CH$_3$)$_3$CP), 30.8 (s, br, 3C, (CH$_3$)$_3$CP), 31.4 (s, br, 1C, (CH$_3$)$_3$CP), 34.9 (s, 1C, (CH$_3$)$_3$CP), 37.1 (d, $^1J_{CP}$ = 4.4 Hz, 1C, (CH$_3$)$_3$CP), 37.7 (d, $J_{CP}$ = 12.9 Hz, 1C, (CH$_3$)$_3$CP), 38.4 (m, $J_{CP}$, 1C, (CH$_3$)$_3$CP), 39.5 (d, $^1J_{CP}$ = 17.6 Hz, 1C, PCH$_2$), 65.4 (d, $^1J_{CP}$ = 20.6 Hz, 1C, PCH), 116.5 (d, br, $^3J_{PC}$ = 3.8 Hz, 1C, C$H_{py}$), 119.9 (d, $^3J_{PC}$ = 5.7 Hz, 1C, C$H_{py}$), 135.2 (s, br, 1C, C$H_{py(4)}$), 159.0 (dd, $^2J_{PC}$ = 15.6 Hz, $^3J_{PC}$ = 5.5 Hz, 1C, C=N), 161.0 (dd, $^2J_{PC}$ = 5.0 Hz, $^3J_{PC}$ = 4.2 Hz, 1C, $C_{py}$), 163.6 (d, br, $^2J_{PC}$ = 1.0 Hz, 1C, $C_{py}$), 211.9 (m, br, $^2J_{CP}$, 1C, Re−CO), 215.4 (m, br, $^2J_{CP}$, 1C, Re−CO) ppm. IR (KBr, pellet) $\nu$ [cm$^{-1}$]: 1800, 1876 ($\nu_{CO}$, 1:1 ratio). Anal. Calcd for $C_{30}H_{51}N_2O_2P_2Re$: C, 50.05; H, 7.14; N, 3.89. C, 49.59; H, 7.29; N, 4.03.

***cis*-[Re(PNP$^{tBu}$−HNC−CHMe)(CO)$_2$] (8).** KO$t$Bu (10 mg, 0.09 mmol, 1 equiv) was added to a stirred solution of **3** (62 mg, 0.09 mmol) in 3 mL of THF in a 20 mL vial. After 20 min, all volatiles were evaporated in vacuo. The residue was extracted in $n$-pentane (15 mL) and filtered through a syringe filter (Teflon, 0.2 $\mu$m pore size). Subsequently, excess propiononitrile was added dropwise (0.5 mL) to the stirred green solution, and a color change to red was observed. The mixture was allowed to stay at −38 °C for 24 h to form large red crystals (suitable for X-ray diffraction analysis). The almost colorless

supernatant solution was decanted, and the obtained product was washed with cold *n*-pentane and dried in vacuo. Yield: 59 mg, 93%. $^{1}$H NMR (500.13 MHz, toluene-$d_8$, 25 °C) ∂: 0.78 (d, br, $^{3}J_{PH}$ = 11.50 Hz, 9H, $(CH_3)_3$CP), 1.06 (d, $^{3}J_{PH}$ = 11.50 Hz, 9H, $(CH_3)_3$CP), 1.47 (d, $^{3}J_{PH}$ = 12.50 Hz, 9H, $(CH_3)_3$CP), 1.63 (d, $^{3}J_{PH}$ = 12.00 Hz, 9H, $(CH_3)_3$CP), 1.64 (d, obscured, $^{3}J_{HH}$, 3H, CH−$CH_3$), 2.38 (s, br, 1H, N*H*), 3.20 (d, $^{2}J_{HH}$ = 15.50 Hz, $^{2}J_{HP}$ = 5.50 Hz, 1H, P$CH_2$), 3.38 (dd, $^{2}J_{HH}$ = 15.50 Hz, $^{2}J_{HP}$ = 9.00 Hz, 1H, P$CH_2$), 4.25 (q, $^{3}J_{HH}$ = 6.50 Hz, 1H, C=*CH*−Me), 4.31 (dt, $^{2}J_{HP}$ = 7.00 Hz, $^{4}J_{HH}$ = 2.00 Hz, 1H, P*CH*), 6.50 (d, $^{3}J_{HH}$ = 7.50 Hz, 1H, $CH_{py}$), 6.79 (d, $^{3}J_{HH}$ = 7.50 Hz, 1H, $CH_{py}$), 6.93 (t, $^{3}J_{HH}$ = 7.50 Hz, 1H, $CH_{py(4)}$) ppm. $^{31}$P{$^{1}$H} NMR (202.5 MHz, toluene-$d_8$, 25 °C) ∂: 84.8 (d, $^{2}J_{PP}$ = 190.4 Hz, 1P, *P*$CH_2$), 95.6 (d, $^{2}J_{PP}$ = 191.9 Hz, 1P, *P*CH(N=C)) ppm. $^{13}$C{$^{1}$H} QDEPT NMR (100.7 MHz, toluene-$d_8$, −65 °C) ∂: 11.7 (s, 1C, $CH_3$), 29.5 (d, br, 3C, $^{3}J$ = 2.4 Hz, $(CH_3)_3$C), 29.9 (s,br, 3C, $(CH_3)_3$CP), 30.2 (d, 3C, $^{3}J$ = 3.3 Hz, $(CH_3)_3$CP), 30.4 (d, 3C, $^{3}J$ = 3.7 Hz, $(CH_3)_3$CP), 36.5 (m, $^{1}J_{CP,}$ $^{3}J_{CP}$ overlay 2C, $(CH_3)_3$CP), 37.7 (d, $J_{CP}$ = 10.0 Hz, 1C, $(CH_3)_3$CP), 37.8 (d, $J_{CP}$ = 20.2 Hz, 1C, $(CH_3)_3$CP), 39.8 (d, $^{1}J_{CP}$ = 18.2 Hz, 1C, P$CH_2$), 63.1 (d, $^{1}J_{CP}$ = 13.9 Hz, 1C, PCH=CN), 78.1 (d, $^{1}J_{CP}$ = 3.8 Hz, 1C, =CH−Me), 117.6 (d, $^{3}J_{PC}$ = 6.3 Hz, 1C, $CH_{py}$), 118.0 (d, $^{3}J_{PC}$ = 7.1 Hz, 1C, $CH_{py}$), 136.4 (s, br, 1C, $CH_{py(4)}$), 150.3 (dd, br, $^{2}J_{PC}$ = 7.5 Hz, $^{4}J_{PC}$ = 2.0 Hz, 1C, C−NH), 161.6 (dd, $^{2}J_{PC}$ = 4.6 Hz, $^{3}J_{PC}$ = 2.2 Hz, 1C, $C_{py}$), 159.0 (dd, $^{2}J_{PC}$ = 7.2 Hz, $^{3}J_{PC}$ = 2.5 Hz, 1C, $C_{py}$), 208.5 (dd, br, $^{2}J_{CP}$ = 8.0 Hz, $^{2}J_{CP}$ = 6.0 Hz, 1C, Re−CO), 208.8 (t, br, $^{2}J_{CP}$ = 5.2 Hz, 1C, Re−CO) ppm. IR (KBr, pellet) $\nu$[cm$^{-1}$]: 1890, 1813 ($\nu_{CO}$, 1:1 ratio). Anal. Calcd for $C_{28}H_{47}N_2O_2P_2Re$: C, 48.61; H, 6.85; N, 4.05. Found: C, 49.28; H, 7.07; N, 3.69.

***cis*-[Re(PNP$^{tBu}$−HNC−CHPh)(CO)$_2$] (9).** KO*t*Bu (10 mg, 0.09 mmol, 1 equiv) was added to a stirred solution of **3** (62 mg, 0.09 mmol) in 3 mL of THF in a 20 mL vial. After 20 min, all volatiles were evaporated in vacuo. The residue was extracted in *n*-pentane (15 mL) and filtered through a syringe filter (Teflon, 0.2 μm pore size). Subsequently, excess benzyl cyanide (1 mL) was added dropwise to the stirred green solution. The red mixture was allowed to stay at −38 °C for 24 h to form a red precipitate. The supernatant solution was decanted, and the obtained product was washed with cold *n*-pentane. Recrystallization from a benzene (3 mL)/*n*-pentane (15 mL) layered solution at −38 °C gave large red crystals (suitable for X-ray diffraction analysis), which were subsequently washed with *n*-pentane and dried in vacuo. Yield: 45 mg, 67%. $^{1}$H NMR (400.36 MHz, toluene-$d_8$, 25 °C) ∂: 0.73 (d, br, $^{3}J_{PH}$ = 11.61 Hz, 9H, $(CH_3)_3$CP), 1.05 (d, $^{3}J_{PH}$ = 12.01 Hz, 9H, $(CH_3)_3$CP), 1.45 (d, $^{3}J_{PH}$ = 12.81 Hz, 9H, $(CH_3)_3$CP), 1.58 (d, $^{3}J_{PH}$ = 12.80 Hz, 9H, $(CH_3)_3$CP), 3.12 (dd, $^{2}J_{HH}$ = 15.61 Hz, $^{2}J_{HP}$ = 5.61 Hz, 1H, P$CH_2$), 3.31 (dd, $^{2}J_{HH}$ = 15.61 Hz, $^{2}J_{HP}$ = 9.20 Hz, 1H, P$CH_2$), 4.41 (dt, $^{2}J_{HP}$ = 6.81 Hz, $J_{HH}$ = 2.00 Hz, 1H, P*CH*), 4.65 (s, br, 1H, N*H*), 5.32 (s, 1H, Ph(*H*)C=C), 6.45 (d, $^{3}J_{HH}$ = 7.60 Hz, 1H, $CH_{py}$), 6.81 (d, $^{3}J_{HH}$ = 8.00 Hz 1H, $CH_{py}$), 6.87 (t, $^{3}J_{HH}$ = 7.21 Hz, 1H, $CH_{Ar}$), 6.92 (t, $^{3}J_{HH}$ = 7.61 Hz, 1H, $CH_{py(4)}$), 7.22 (t, $^{3}J_{HH}$ = 7.61 Hz, 2H, $CH_{Ar}$), 7.34 (d, $^{3}J_{HH}$ = 7.21 Hz, 2H, $CH_{Ar}$) ppm. $^{31}$P{$^{1}$H} NMR (162.1 MHz, toluene-$d_8$, 25 °C) ∂: 82.9 (d, $^{2}J_{PP}$ = 186.7 Hz, 1P), 98.9 (d, $^{2}J_{PP}$ = 186.6, 1P) ppm. $^{13}$C{$^{1}$H} QDEPT NMR (100.7 MHz, toluene-$d_8$, 25 °C) ∂: 29.5 (d, br, 3C, $^{2}J_{CP}$ = 4.1 Hz $(CH_3)_3$C), 30.0 (d, br, 3C, $^{2}J_{CP}$ = 3.1 Hz $(CH_3)_3$C), 30.4 (2d, br, obscured, 6C, $J_{CP}$, $(CH_3)_3$C), 36.4 (dd, $^{1}J_{CP}$ = 7.8 Hz, $^{3}J_{CP}$ = 5.5 Hz, 1C, $(CH_3)_3$CP), 36.8 (dd, $^{1}J_{CP}$ = 11.7 Hz, $^{3}J_{CP}$ = 1.7 Hz, 1C, $(CH_3)_3$CP), 37.4 (d, $^{1}J_{CP}$ = 9.4 Hz, 1C, $(CH_3)_3$CP), 38.0 (d, $^{1}J_{CP}$ = 20.3 Hz, 1C, $(CH_3)_3$CP), 39.9 (d, $^{1}J_{CP}$ = 18.0 Hz, 1C, P$CH_2$), 65.7 (d, $^{1}J_{CP}$ = 13.1 Hz, 1C, PCH), 90.5 (d, $^{3}J_{CP}$ = 3.7 Hz, 1C, Ph(H)C=*C*), 118.0 (d, br, $^{3}J_{PC}$ = 6.1 Hz, 1C, $CH_{py}$), 118.2 (d, $^{3}J_{PC}$ = 6.9 Hz, 1C, $CH_{py}$), 120.1 (s, 1C, $CH_{Ar,para}$), 123.7 (s, 2C, $CH_{Ar,ortho}$), 128.2 (s, 2C, $CH_{Ar,meta}$), 136.6 (s, 1C, $CH_{py(4)}$), 142.9 (s, 1C, $C_{Ar,\ ipso}$), 153.5 (dd, $^{2}J_{PC}$ = 8.2 Hz, $^{4}J_{PC}$ = 2.0 Hz, 1C, C−NH), 162.1 (dd, $^{2}J_{PC}$ = 4.3 Hz,, $^{3}J_{PC}$ = 1.9 Hz, 1C, $C_{py}$), 162.1 (dd, $^{2}J_{PC}$ = 6.8 Hz,, $^{3}J_{PC}$ = 3.1 Hz, 1C, $C_{py}$), 208.2 (t, $^{2}J_{CP}$,= 5.0 Hz, 1C, Re−CO), 208.4 (t, $^{2}J_{CP}$ = 6.5 Hz, 1C, Re−CO) ppm. IR (KBr, pellet) $\nu$ [cm$^{-1}$]: 1899, 1821 ($\nu_{CO}$, 1:1 ratio). Anal. Calcd for $C_{33}H_{49}N_2O_2P_2Re$: C, 52.57; H, 6.55; N, 3.72. Found: C, 53.21; H, 6.29; N, .

***cis*-[Re(PNP$^{tBu}$−N(Me)=CPh$^{pCF3}$)(CO)$_2$]OTf (10).** Complex **6** (27 mg, 0.03 mmol) was dissolved in 3 mL of benzene in a 20 mL vial. Excess methyl triflate (5 drops via Pasteur pipet) was added to the stirred red solution until a color change to yellow was evident. After 15 min at ambient temperature, *n*-pentane was added to the mixture to precipitate a yellow-orange solid, which was washed with *n*-pentane (5 mL) and dried in vacuo. Subsequently, the yellow residue was dissolved in methylene chloride (3 mL), layered with *n*-pentane (15 mL), and allowed to crystallize for 24 h at ambient temperature. The obtained orange crystals (suitable for X-ray diffraction analysis) were washed with *n*-pentane and dried in vacuo. Yield 30 mg, 92%. $^{1}$H NMR (500.13 MHz, acetone-$d_6$, 25 °C) ∂: 1.11 (s, br, partly obscured, 9H, $(CH_3)_3$CP), 1.16 (d, $^{3}J_{PH}$ = 13.00 Hz, 9H, $(CH_3)_3$CP), 1.66 (d, $^{3}J_{PH}$ = 13.00 Hz, 9H, $(CH_3)_3$CP), 1.70 (d, $^{3}J_{PH}$ = 13.50 Hz, 9H, $(CH_3)_3$CP), 3.86 (dd, $^{2}J_{HH}$ = 16.50 Hz, $^{2}J_{HP}$ = 6.00 Hz, 1H, P$CH_2$), 3.97 (s, 3H, N$CH_3$), 4.65 (ddd, $^{2}J_{HH}$ = 16.50 Hz, $^{2}J_{HP}$ = 9.50 Hz, $J$ = 1.00 Hz, 1H, P$CH_2$), 6.61 (dd, $^{2}J_{HP}$ = 6.50 Hz, $J$ = 2.50 Hz, 1H, P*CH*), 7.73 (d, $^{3}J_{HH}$ = 8.00 Hz, 2H, $CH_{Ar}$), 7.96 (m, $J_{HP}$, $J_{HH}$, 4H, overlay $CH_{py}$ + $CH_{Ar}$), 8.14 (t, $^{3}J_{HH}$ = 8.00 Hz, 1H, $CH_{py(4)}$) ppm. $^{31}$P{$^{1}$H} NMR (202.5 MHz, acetone-$d_6$, 25 °C) ∂: 89.3 (d, $^{2}J_{PP}$ = 164.4 Hz, 1P), 149.7 (d, $^{2}J_{PP}$ = 165.0 Hz, 1P) ppm. $^{13}$C{$^{1}$H} QDEPT NMR (125.8 MHz, acetone-$d_6$, 25 °C) ∂: one resonance for $(CH_3)_3$CP) overlaid by acetone residual solvent peak, 30.2 (s, br, 3C, $(CH_3)_3$CP), 30.4 (d, br, $^{2}J_{CP}$ = 3.3 Hz, 3C, $(CH_3)_3$CP), 31.4 (d, br, 3C, $^{2}J_{CP}$ = 3.5 Hz, $(CH_3)_3$CP), 37.5 (dd, $^{1}J_{CP}$ = 8.3 Hz, $^{3}J_{CP}$ = 5.4 Hz, 1C, $(CH_3)_3$CP), 39.0 (d, $J_{CP}$ = 16.4 Hz, 1C, $(CH_3)_3$CP), 39.7 (d, obscured, 1C, $(CH_3)_3$CP), 39.8 (d, $^{1}J_{CP}$ = 20.8 Hz, 1C, P$CH_2$), 40.3 (d, $^{1}J_{CP}$ = 3.1 Hz, 1C, $(CH_3)_3$CP), 52.6 (s, 1C, N−$CH_3$), 66.3 (d, $^{1}J_{CP}$ = 6.8 Hz, 1C, PCH), 122.3 (d, $^{3}J_{PC}$ = 4.8 Hz, 1C, $CH_{py}$), 122.9 (d, $^{3}J_{PC}$ = 6.7 Hz, 1C, $CH_{py}$), 125.1 (q, very weak, (partially obscured) 1C, $CF_3$), 126.6 (q, br, $^{3}J_{FC}$ = 3.5 Hz, 2C, $CH_{Ar}$), 130.0 (s, 2C, $CH_{Ar}$), 132.6 (d, $^{2}J_{FC}$ = 33.1 Hz, 1C, $C_{Ar}$), 136.5 (s, 1C, $C_{Ar}$), 141.2 (s, 1C, $CH_{py}$), 158.9 (dd, $^{2}J_{PC}$ = 7.4 Hz, $^{3}J_{PC}$ = 4.2 Hz, 1C, $C_{py}$), 166.5 (s, br, 1C, $C_{py}$) 178.8 (d, br, $^{2}J_{PC}$ = 7.9 Hz, 1C, *C*=N(Me)), 207.4 (m, br, $^{2}J_{CP}$, 1C, Re−CO), 209.8 (s, br, 1C, Re−*C*O) ppm. $^{19}$F{$^{1}$H} NMR (282.4 MHz, acetone-$d_6$, 25 °C) ∂: −79.6 (s, 3F, $O_3SCF_3$), 64.6 (s, 3F, $CF_3$) ppm. IR (KBr, pellet) $\nu$ [cm$^{-1}$]: 1925, 1851 ($\nu_{CO}$, 1:1 ratio). Anal. Calcd for $C_{35}H_{49}F_6N_2O_5P_2ReS$: C, 43.25; H, 5.08; N, 2.8. Found: C, 44.76; H, 5.43; N, 2.51.

***cis*-[Re(PNP$^{tBu}$−HN=C−CH(Me)Ph)(CO)$_2$]OTf (11).** Complex **9** (45 mg, 0.06 mmol) was dissolved in 4 mL of benzene in a 20 mL vial. Methyl triflate (MeOTf) was added dropwise to the blood-red solution until a color change to yellow was observed (3 drops via Pasteur pipet). *n*-Pentane (5 mL) was added to the solution to precipitate a yellow solid, which was decanted and dissolved in a minimum of THF. Subsequent precipitation with *n*-pentane gave the desired product **11** as a yellow microcrystalline powder, which was separated from the supernatant solution by decantation and dried in vacuo. Yield: 50 mg, 91%. Single crystals suitable for X-ray diffraction analysis were obtained from a concentrated solution in benzene. $^{1}$H NMR (500.13 MHz, $CD_3CN$, 25 °C) ∂: 0.73 (d, br, $^{3}J_{PH}$ = 12.50 Hz, 9H, $(CH_3)_3$CP), 1.11 (d, $^{3}J_{PH}$ = 12.50 Hz, 9H, $(CH_3)_3$CP), 1.44 (d, $^{3}J_{PH}$ = 13.50 Hz, 9H, $(CH_3)_3$CP), 1.47 (d, $^{3}J_{HH}$ = 7.00 Hz, 3H, $CH_3$), 1.53 (d, $^{3}J_{PH}$ = 13.50 Hz, 9H, $(CH_3)_3$CP), 3.57 (dd, $^{2}J_{HH}$ = 17.00 Hz, $^{2}J_{HP}$ = 5.50 Hz, 1H, P$CH_2$), 3.31 (ddd, $^{2}J_{HH}$ = 16.80 Hz, $^{2}J_{HP}$ = 10.00 Hz, $J$ = 1.00 Hz, 1H, P$CH_2$), 4.45 (q, $^{3}J_{HH}$ = 7.00 Hz, 1H, (Me)C*H*), 4.41 (dt, $^{2}J_{HP}$ = 6.50 Hz, $^{4}J_{HH}$ = 1.50 Hz, 1H, P*CH*), 7.13 (d, $^{3}J_{HH}$ = 8.00 Hz, 2H, $CH_{Ar}$), 7.42 (m, $J_{HH}$, overlaid, 3H, $CH_{Ar}$), 7.61 (d, $^{3}J_{HH}$ = 8.00 Hz, 1H, $CH_{py}$), 7.90 (d, $^{3}J_{HH}$ = 7.50 Hz, 1H, $CH_{py}$), (t, $^{3}J_{HH}$ = 8.00 Hz, 1H, $CH_{py(4)}$), 9.96 (s, br, 1H, C=N*H*) ppm. $^{31}$P{$^{1}$H} NMR (202.5 MHz, $CD_3CN$ 25 °C) ∂: 88.9 (d, $^{2}J_{PP}$ = 162.6 Hz, 1P), 147.5 (d, $^{2}J_{PP}$ = 166.2, 1P) ppm. $^{13}$C{$^{1}$H} QDEPT NMR (125.8 MHz, $CD_3CN$, 25 °C) ∂: 18.0 (s, 1C, $CH_3$), 29.2 (d, br, 3C, $^{2}J_{CP}$ = 4.3 Hz $(CH_3)_3$C), 29.8 (d, br, 3C, $^{2}J_{CP}$ = 2.1 Hz $(CH_3)_3$C), 30.2 (2 d, br, $^{2}J_{CP}$ = 3.6 Hz, 3C, $(CH_3)_3$C), 30.7 (2 d, $^{2}J_{CP}$ = 3.9 Hz, 3C, $(CH_3)_3$C), 37.6 (dd, $^{1}J_{CP}$ = 11.2 Hz, $^{3}J_{CP}$ = 4.9 Hz, 1C, $(CH_3)_3$CP), 38.8 (d, $^{1}J_{CP}$ = 21.6 Hz, partly overlaid, 1C, $(CH_3)_3$CP), 38.9 (dd, $^{1}J_{CP}$ = 14.5 Hz, $^{3}J_{CP}$ = 1.3 Hz, 1C, $(CH_3)_3$CP), 39.4 (m, partly obscured, $J_{CP}$ = 3.8 Hz, 1C, $(CH_3)_3$CP), 39.6 (d, $^{1}J_{CP}$ = 20.5 Hz, 1C, P$CH_2$), 50.0 (d, $^{3}J_{CP}$ = 1.8 Hz, 1C, (Me)CH), 61.4 (d, $^{1}J_{CP}$ = 5.2 Hz, 1C, PCH), 122.1 (d, $^{3}J_{PC}$ = 7.0 Hz, 1C, $CH_{py}$), 123.1 (d, $^{3}J_{PC}$ = 6.9 Hz, 1C, $CH_{py}$), 129.0 (s, 2C,


dx.doi.org/10.1021/ja4071859 | J. Am. Chem. Soc. 2013, 135, 17004−17018

$CH_{Ar}$), 129.1 (s, 1C, $CH_{Ar,para}$), 129.9 (s, 2C, $CH_{Ar}$), 137.0 (s, 1C, $C_{Ar,ipso}$), 140.1 (s, 1C, $CH_{py(4)}$), 158.5 (dd, $^2J_{PC}$ = 6.4 Hz,, $^3J_{PC}$ = 4.5 Hz, 1C, $C_{py}$), 165.8 (t, br, $^2J_{PC}$ = 2.6 Hz, 1C, $C_{py}$), 189.7 (dd, $^2J_{PC}$ = 8.2 Hz,, $^4J_{PC}$ = 2.9 Hz, 1C, *C*=NH), 208.0 (m, $J_{CP}$, 2C, superimposed Re−CO moieties) ppm. $^{19}F\{^1H\}$ NMR (282.4 MHz, $CD_3CN$, 25 °C) $\partial$: −80.1 (s, 3F, $O_3SCF_3$), 64.6 (s, 3F, $CF_3$) ppm. IR (KBr, pellet) $\nu$ [$cm^{-1}$]: 1921, 1851 ($\nu_{CO}$, 1:1 ratio). Anal. Calcd for $C_{35}H_{52}F_3N_2O_5P_2ReS$: C, 45.79; H, 5.71; N, 3.05. Found: C, 46.29; H, 5.70; N, 2.50.

***mer*-[Re(PNP$^{tBu}$*)(CO)$_3$] (12).** In an experiment performed in a J. Young NMR tube fitted with a Kontes valve, complex **9** (10 mg, 0.01 mmol) was dissolved in 0.5 mL of $C_6D_6$. The red solution was degassed in a freeze−pump−thaw cycle and pressurized with 1 atm of CO gas. After 15 min at ambient temperature, ∼10% of complex **12** was formed. The reaction was brought to completion by heating the NMR tube for 1 h at 65 °C in an oil bath. To verify the nature of **12** as *mer*-[Re(PNP$^{tBu}$*)(CO)$_3$], a control experiment was performed in a J. Young NMR tube fitted with a Kontes valve: The dearomatized complex **4** (10 mg, 0.015 mmol) was dissolved in 0.5 mL of $C_6D_6$ and pressurized with 1 atm CO gas. The initial green solution turned instantly yellow to form **12** quantitatively. $^1H$ NMR (300.13 MHz, $C_6D_6$, 25 °C) $\partial$: 1.09 (d, $^3J_{PH}$ = 13.20 Hz, 18H, $(CH_3)_3CP$), 1.44 (d, $^3J_{PH}$ = 13.20 Hz, 18H, $(CH_3)_3CP$), 2.83 (d, $^2J_{HH}$ = 8.10 Hz, 1H, $PCH_2$), 4.01 (s, br, 1H, PC*H*), 5.46 (d, $^3J_{HH}$ = 6.30 Hz, 1H, $CH_{py}$), 6.31 (d, $^3J_{HH}$ = 8.70 Hz, 1H, $CH_{py}$), 6.44 (t, br, $^3J_{HH}$ = 8.10 Hz, 1H, $CH_{py(4)}$) ppm. $^{31}P\{^1H\}$ NMR (121.5 MHz, $C_6D_6$, 25 °C) $\partial$: 53.2 (d, $^2J_{PP}$ = 113.2 Hz, 1P), 67.2 (d, $^2J_{PP}$ = 117.5 Hz, 1P) ppm. $^{13}C\{^1H\}$ QDEPT NMR (100.7 MHz, $C_6D_6$, 25 °C) $\partial$: 29.8 (d, $^2J_{PC}$ = 3.7 Hz, 6C, $(CH_3)_3CP$), 30.6 (d, $^2J_{PC}$ = 3.8 Hz, 6C, $(CH_3)_3CP$), 37.2 (d, $^1J_{CP}$ = 17.6 Hz, 2C, $(CH_3)_3CP$), 39.2 (d, $^1J_{CP}$ = 24.3 Hz, 2C, $(CH_3)_3CP$), 39.9 (d, $^1J_{CP}$ = 29.7 Hz, 1C, PCH), 69.5 (d, $^1J_{CP}$ = 50.5 Hz, 1C, $PCH_2$), 100.3 (d, $^3J_{PC}$ = 8.3 Hz, 1C, $CH_{py}$), 113.7 (d, $^3J_{PC}$ = 15.4 Hz, 1C, $CH_{py}$), 131.2 (s, 1C, $CH_{py(4)}$), 157.9 (s, br, 1C, $C_{py}$), 172.5 (dd, $^2J_{PC}$ = 14.0 Hz, $^3J_{PC}$ = 3.2 Hz, 1C, $C_{py}$), 199.4 (t, $^2J_{CP}$ = 7.9 Hz, 2C, Re−CO), 202.0 (m, br, $^2J_{CP}$ 1C, Re−CO) ppm.

**Deprotonation of 11 To Form (i-*E* and -*Z*) and Formation of 9 via Addition of Benzyl Cyanide (Scheme 4).** Complex **11** (27 mg, 0.03 mmol) was suspended in toluene-$d_8$ (1 mL) in a 20 mL vial, and KO$^t$Bu (4 mg, 1.3 equiv) was added to the vigorously stirred mixture. The greenish solution was filtered through a syringe filter (Teflon, 0.2 $\mu$m pore size) and transferred to a J. Young NMR tube and investigated in situ by NMR spectroscopy. Addition of excess benzyl cyanide (10 $\mu$L, $d_{20}$ = 1.02 g/cm$^3$, 3 equiv) via microsyringe gave complex **9** and free 2-phenylpropanenitrile, which was identified by GC−MS analysis.

**Catalyzed Michael Additions− Experiments of Table 3.** *General Procedure.* The specific benzyl cyanide derivative (amounts are specified in Table 3) was dissolved in 0.5 mL of THF in a 20 mL vial, and 1 equiv of the specific acceptor was dissolved in 0.5 mL of THF and added to the cyanide solution. The catalyst (2 mol %, complex **9** or **4**, respectively, as specified) was added to the substrate mixture, and the solution was transferred to a Schlenk tube and heated in an oil bath to the specified temperature for the indicated time period. After the reaction vessel was cooled to room temperature, all volatiles were evaporated in vacuo. The resulting residue was dissolved in $CDCl_3$. An appropriate standard was added to the solution to determine the yields via $^1H$ NMR spectroscopy via relative comparison of the integration values with standard compound. For details, see the Supporting Information. The product was purified for NMR characterization using a preparative TLC sheet (scale, 15−30 mg of compound; eluent, *n*-hexane:ethyl acetate 4:1).

**Methyl 4-Cyano-4-phenylbutanoate (13).** $^1H$ NMR (500.13 MHz, $CDCl_3$, 25 °C): 2.15 (q, $^3J_{HH}$ = 7.4 Hz, 2H, $(CH_2)CHCN$), 2.42 (m, 2H, $CH_2$)C=O), 3.60 (s, 3H, $OCH_3$), 3.90 (t, $^3J_{HH}$ = 7.5 Hz, 1H, *CHCN*), 7.27 (br, 3H, $C_6H_5$), 7.30 (br, 2H, $C_6H_5$). $^{13}C\{^1H\}$ QDEPT NMR (125.8 MHz, $CDCl_3$, 25 °C): 30.80 (s, 1C, $CH_2C$=O), 30.83 (s, 1C $(CH_2)CHCN$), 36.35 (s, 1C, *C*HCN), 51.95 (s, 1C, $OCH_3$), 120.32 (s, 1C, *C*N), 127.37 (s, 2C, $CH_{ar}$), 128.40 (s, 1C, $CH_{ar}$), 129.27 (s, 2C, $CH_{ar}$), 135.02 (*s*, 1C, $C_6H_5$-*ipso*), 172.55 (s, 1C, C=O).

**Phenyl 4-Cyano-4-phenylbutanoate (15).** $^1H$ NMR (500.13 MHz, $CDCl_3$, 25 °C): 2.26 (q, $^3J_{HH}$ = 7.4 Hz, 2H, $(CH_2)CHCN$), 2.67 (m, 2H, $(CH_2)$C=O), 3.98 (t, $^3J_{HH}$ = 7.4 Hz, 1H, *CH*CN), 6.98 (d, 2H, $C_6H_{5(acrylate)}$), 7.18 (br, 1H, $CH_{ar\ (cyanide)}$), 7.31 (m, 7H, $CH_{ar\ (acrylate+cyanide)}$). $^{13}C\{^1H\}$ QDEPT NMR (125.8 MHz, $CDCl_3$, 25 °C): 31.00 (s, 1C, $(CH_2)CHCN$), 31.43 (s, 1C, (CH2)C=O), 36.63 (s, 1C, *C*HCN), 120.56 (s, 1C, *C*N), 121.77 (s, 2C, $CH_{ar\ 5(acrylate-ortho)}$), 126.43 (s, 1C, $CH_{ar5}$), 127.69 (s, 2C, $CH_{ar}$), 128.81 (s, 1C, $CH_{ar5}$), 129.66 (s, 2C, $CH_{ar}$), 129.88 (s, 2C, $CH_{ar}$), 135.18 (s, 1C, $C_6H_5$-*ipso*) 150.71 (s, 1C, $C_6H_5$-*ipso*), 171.09 (s, 1C, *C*=O).

**5-Oxo-2-phenylhexanenitrile (16).** $^1H$ NMR (500.13 MHz, $CDCl_3$, 25 °C): 2.09 (s, 3H, $(CH_3)$C=O), 2.10 (m, 2H, $(CH_2)CHCN$), 2.52 (ddd, $^{2,3}J_{HH}$ = 18.5, 7.3, 5.9 Hz, 1H, $(CH_2)$C=O), 2.58 (dvt, $^{2,3}J_{HH}$ = 18.4, 7.4 Hz, 1H, $(CH_2)$C=O), 3.88 (dd, $^3J_{HH}$ = 8.8 Hz, $^3J_{HH}$= 6.2 Hz, 1H, *CH*CN), 7.27 (br, 3H, $C_6H_5$), 7.30 (br, 2H, $C_6H_5$). $^{13}C\{^1H\}$ QDEPT NMR (125.8 MHz, $CDCl_3$, 25 °C): 29.78 (s, 1C, $CH_2CHCN$), 30.48 (s, 1C, $CH_3$), 36.46 (s, 1C, *C*HCN), 40.25 (s, 1C, $(CH_2)$C=O), 120.81 (s, 1C, *C*N), 127.6 (s, 2C, $CH_{ar}$), 128.61 (s, 1C, $CH_{ar}$), 129.53 (s, 2C, $CH_{ar}$), 135.57 (s, 1C, $C_6H_5$-*ipso*), 207.21 (s, 1C, *C*=O).

**2-(3-Oxocyclohexyl)-2-phenylacetonitrile (17).** The product was obtained as a 1:1 diastereomeric mixture. Analytical data have been previously reported.[82]

**Methyl 4-(4-Aminophenyl)-4-cyanobutanoate (18).** $^1H$ NMR (300.13 MHz, $CDCl_3$, 25 °C): 2.11 (dd, $^3J_{HH}$ = 7.0, 14.2 Hz, 2H, $(CH_2)CHCN$), 2.40 (m, 2H, $(CH_2)$C=O), 3.56 (s, 2H, $NH_2$), 3.61 (s, 3H, $OCH_3$), 3.77 (t, $^3J_{HH}$ = 7.3 Hz, 1H, *CH*CN), 6.60 (d, $^3J_{HH}$ = 7.9 Hz, 2H, $C_6H_4$−$NH_2$), 7.03 (d, $^3J_{HH}$ = 7.8 Hz, 2H, $C_6H_4$−$NH_2$). $^{13}C\{^1H\}$ QDEPT NMR (100.7 MHz, $CDCl_3$, 25 °C): 30.92 (s, 2C, $CH_2$), 35.65 (s, 1C, *C*HCN), 51.95 (s, 1C, $OCH_3$), 115.61 (s, 2C, $C_6H_4$−$NH_2$), 120.86 (s, 1C, *C*N), 124.54 (s, 1C, $C_6H_4$-*ipso*), 128.42 (s, 2C, $C_6H_4$−$NH_2$), 146.55 (s, 1C, $C_6H_4$-*ipso*), 172.74 (s, 1C, C=O).

**Methyl 4-(3-Bromophenyl)-4-cyanobutanoate (19).** $^1H$ NMR (300.13 MHz, $CDCl_3$, 25 °C): 2.14 (m, 2H, $(CH_2)CHCN$), 2.44 (m, 2H, $(CH_2)$C=O), 3.63 (s, 3H, $CH_3$), 3.90 (t, $^3J_{HH}$ = 7.54 Hz, 1H, *CH*CN), 7.20 (m, 2H, $C_6H_4$−Br), 7.42 (m, 2H, $C_6H_4$−Br). $^{13}C\{^1H\}$ QDEPT NMR (100.7 MHz, $CDCl_3$, 25 °C): 30.76 (s, 2C, $CH_2$), 36.00 (s, 1C, *C*HCN), 52.05 (s, 1C, $OCH_3$), 119.67 (s, 1C, CN), 123.28 (s, 1C, $C_6H_4$-ipso), 126.09 (s, 1C, $CH_{ar}$), 130.50 (s, 1C, $CH_{ar}$), 130.86 (s, 1C, $CH_{ar}$), 131.7 (s, 1C, $CH_{ar}$), 137.28 (s, 1C, $C_6H_4$-*ipso*), 172.40 (s, 1C, *C*=O).

**Double Additions of Methyl Acrylate to Benzyl Cyanide.** Complex **9** (5 mg, 0.0066 mmol, 1 mol %) dissolved in 1 mL of THF was added to a solution of benzyl cyanide (78 mg, 0.66 mmol) and methyl acrylate (120 mg, 1.4 mmol, 2 equiv) in 1 mL of THF. The mixture was heated in a closed Schlenk tube at 80 °C for 12 h. After the reaction vessel was cooled to room temperature, all volatiles were removed in vacuo to yield dimethyl 4-cyano-4-phenylheptanedioate (**14**) in quantitative yield (NMR). Alternatively, **14** was obtained via the stepwise addition of 2 equiv of methyl acrylate. Benzyl cyanide (47 mg, 0.4 mmol) was dissolved in 0.5 mL of THF in a 20 mL vial; 1 equiv of methyl acrylate (35 mg, 0.4 mmol) was dissolved in 0.5 mL of THF and added to the benzyl cyanide solution. The catalyst (complex **9**, 6 mg, 0.008 mmol, 2 mol %) was added to the substrate mixture, and the solution was transferred to a Schlenk tube and heated in an oil bath at 65 °C for 20 h. Subsequently, another equivalent of methyl acrylate (35 mg, 0.4 mmol) was added, and the mixture was heated at 80 °C for another 10 h. After the reaction vessel was cooled to room temperature, a sample was taken for GC analysis. Conversion with respect to methyl acrylate was >99% GC. Quantitative formation gave dimethyl 4-cyano-4-phenylheptanedioate (**14**).

**Dimethyl 4-Cyano-4-phenylheptanedioate (14).** $^1H$ NMR (500.13 MHz, $C_6D_6$, 25 °C): 1.94 (m, 6H, $(CHHCH_2)$C=O), 2.30 (m, 2H, $(CHH, CH_2)$C=O), 3.20 (s, 6H, $OCH_3$), 6.93 (br, 3H, $C_6H_5$), 7.07 (dd, $^3J_{HH}$ = 8.0 Hz, 2H, $C_6H_5$). $^{13}C\{^1H\}$ QDEPT NMR (125.8 MHz, $C_6D_6$, 25 °C): 30.12 (s, $CH_2$C=O), 35.81 (s, $(CH_2)CHCN$), 46.93 (s, *C*CN), 51.13 (s, $OCH_3$), 121.06 (s, *C*N), 126.09 (s, $CH_{ar}$), 128.12 (s, $CH_{ar}$), 129.30 (s, $CH_{ar}$), 137.04 (*s*, $C_6H_5$-*ipso*), 171.79 (*C*=O).


dx.doi.org/10.1021/ja4071859 | J. Am. Chem. Soc. 2013, 135, 17004−17018

**Control Experiments.** *Complex 4 as Catalyst.* Benzyl cyanide (47 mg, 0.4 mmol) was dissolved in 0.5 mL of THF in a 20 mL vial, and 1 equiv of methyl acrylate (35 mg, 0.4 mmol) was dissolved in 0.5 mL of THF and added to the cyanide solution. Complex **4** (5.5 mg, 0.008 mmol, 2 mol %) was added to the substrate mixture, and the solution was transferred to a Schlenk tube and heated in an oil bath for 20 h at 65 °C. After the reaction vessel was cooled to room temperature, all volatiles were evaporated in vacuo. The resulting residue was dissolved in $CDCl_3$. Ferrocene as standard was added to the solution to determine the yields via $^1H$ NMR spectroscopy via relative comparison of the integration values with standard compound. Yield: 87%. Catalytic use of KO$^t$Bu: Benzyl cyanide (47 mg, 0.4 mmol) was dissolved in 0.5 mL of THF in a 20 mL vial; 1 equiv of methyl acrylate (35 mg, 0.4 mmol) was dissolved in 0.5 mL of THF and added to the benzyl cyanide solution. Potassium *tert*-butoxide (1 mg, 0.008 mmol, 2 mol %) was added to the substrate mixture, and the solution was transferred to a Schlenk tube and heated in an oil bath for 20 h at 65 °C. After the reaction vessel was cooled to room temperature, all volatiles were evaporated in vacuo. The resulting residue was dissolved in $CDCl_3$. Ferrocene as a standard was added to the solution to determine the yields via $^1H$ NMR spectroscopy via relative comparison of the integration values with standard compound. Conversion with respect to methyl acrylate was >99% GC. Yield of products: 37% (**13**), 26% (**14**), and nonidentified byproducts.

## ■ ASSOCIATED CONTENT

### Ⓢ Supporting Information

Figures giving NMR spectra, coordinates for the DFT optimized geometries, and CIF files for all structures. This material is available free of charge via the Internet at http://pubs.acs.org.

## ■ AUTHOR INFORMATION


### Corresponding Author

david.milstein@weizmann.ac.il

### Author Contributions

[§]These authors contributed equally.


### Notes

The authors declare no competing financial interest.

## ■ ACKNOWLEDGMENTS

This research was supported by the European Research Council under the FP7 framework (ERC No. 246837). D.M. holds the Israel Matz Professorial Chair of Organic Chemistry. M.V. would like to thank the Swiss Friends of the Weizmann Institute for a postdoctoral fellowship.

## ■ REFERENCES


(1) Albrecht, M.; Lindner, M. M. *Dalton Trans.* **2011**, *40*, 8733.
(2) Albrecht, M.; van Koten, G. *Angew. Chem., Int. Ed.* **2001**, *40*, 3750−3781.
(3) Gunanathan, C.; Milstein, D. *Acc. Chem. Res.* **2011**, *44*, 588−602.
(4) Gunanathan, C.; Milstein, D. *Top. Organomet. Chem.* **2011**, *37*, 55−84.
(5) van der Vlugt, J. I. *Eur. J. Inorg. Chem.* **2012**, *2012*, 363−375.
(6) van der Vlugt, J. I.; Reek, J. N. H. *Angew. Chem., Int. Ed.* **2009**, *48*, 8832−8846.
(7) *The Chemistry of Pincer Compounds*; Morales-Morales, D., Jensen, M. C., Eds.; Elsevier: New York, 2007; pp 1−467.
(8) van der Vlugt, J. I.; Pidko, E. A.; Bauer, R. C.; Gloaguen, Y.; Rong, M. K.; Lutz, M. *Chem.-Eur. J.* **2011**, *17*, 3850−3854.
(9) van der Vlugt, J. I.; Lutz, M.; Pidko, E. A.; Vogt, D.; Spek, A. L. *Dalton Trans.* **2009**, 1016−1023.
(10) Feller, M.; Diskin-Posner, Y.; Shimon, L. J. W.; Ben-Ari, E.; Milstein, D. *Organometallics* **2012**, *31*, 4083−4101.
(11) Khaskin, E.; Iron, M. A.; Shimon, L. J. W.; Zhang, J.; Milstein, D. *J. Am. Chem. Soc.* **2010**, *132*, 8542−8543.
(12) Kohl, S. W.; Weiner, L.; Schwartsburd, L.; Konstantinovski, L.; Shimon, L. J. W.; Ben-David, Y.; Iron, M. A.; Milstein, D. *Science* **2009**, *324*, 74−77.
(13) Schwartsburd, L.; Iron, M. A.; Konstantinovski, L.; Ben-Ari, E.; Milstein, D. *Organometallics* **2011**, *30*, 2721−2729.
(14) Schwartsburd, L.; Iron, M. A.; Konstantinovski, L.; Diskin-Posner, Y.; Leitus, G.; Shimon, L. J. W.; Milstein, D. *Organometallics* **2010**, *29*, 3817−3827.
(15) Ben-Ari, E.; Leitus, G.; Shimon, L. J. W.; Milstein, D. *J. Am. Chem. Soc.* **2006**, *128*, 15390−15391.
(16) Prechtl, M. H. G.; Hölscher, M.; Ben-David, Y.; Theyssen, N.; Loschen, R.; Milstein, D.; Leitner, W. *Angew. Chem., Int. Ed.* **2007**, *46*, 2269−2272.
(17) Kloek, S. M.; Heinekey, D. M.; Goldberg, K. I. *Angew. Chem., Int. Ed.* **2007**, *46*, 4736−4738.
(18) Hanson, S. K.; Heinekey, D. M.; Goldberg, K. I. *Organometallics* **2012**, *27*, 1454−1463.
(19) de Boer, S. Y.; Gloaguen, Y.; Lutz, M.; van der Vlugt, J. I. *Inorg. Chim. Acta* **2012**, *380*, 336−342.
(20) Hunsicker, D. M.; Dauphinais, B. C.; Mc Ilrath, S. P.; Robertson, N. J. *Macromol. Rapid Commun.* **2011**, *33*, 232−236.
(21) Friedrich, A.; Schneider, S. *ChemCatChem* **2009**, *1*, 72−73.
(22) Zhang, J.; Leitus, G.; Ben-David, Y.; Milstein, D. *J. Am. Chem. Soc.* **2005**, *127*, 10840−10841.
(23) Srimani, D.; Balaraman, E.; Gnanaprakasam, B.; Ben-David, Y.; Milstein, D. *Adv. Synth. Catal.* **2012**, *354*, 2403−2406.
(24) Balaraman, E.; Khaskin, E.; Leitus, G.; Milstein, D. *Nat. Chem.* **2013**, *5*, 122−125.
(25) Gunanathan, C.; Ben-David, Y.; Milstein, D. *Science* **2007**, *317*, 790−792.
(26) Gnanaprakasam, B.; Milstein, D. *J. Am. Chem. Soc.* **2011**, *133*, 1682−1685.
(27) Zeng, H.; Guan, Z. *J. Am. Chem. Soc.* **2011**, *133*, 1159−1161.
(28) Gnanaprakasam, B.; Zhang, J.; Milstein, D. *Angew. Chem., Int. Ed.* **2010**, *49*, 1468−1471.
(29) Michlik, S.; Kempe, R. *Nat. Chem.* **2013**, *5*, 140−144.
(30) Srimani, D.; Ben-David, Y.; Milstein, D. *Angew. Chem., Int. Ed.* **2013**, *52*, 4012−4015.
(31) Gunanathan, C.; Gnanaprakasam, B.; Iron, M. A.; Shimon, L. J. W.; Milstein, D. *J. Am. Chem. Soc.* **2010**, *132*, 14763−14765.
(32) Gunanathan, C.; Milstein, D. *Angew. Chem., Int. Ed.* **2008**, *47*, 8661−8664.
(33) Zhang, J.; Leitus, G.; Ben-David, Y.; Milstein, D. *Angew. Chem. Int. Ed.* **2006**, *45*, 1113−1115.
(34) Balaraman, E.; Fogler, E.; Milstein, D. *Chem. Commun.* **2012**, *48*, 1111−1113.
(35) Balaraman, E.; Gnanaprakasam, B.; Shimon, L. J. W.; Milstein, D. *J. Am. Chem. Soc.* **2010**, *132*, 16756−16758.
(36) Balaraman, E.; Gunanathan, C.; Zhang, J.; Shimon, L. J. W.; Milstein, D. *Nat. Chem.* **2011**, *3*, 609−614.
(37) Balaraman, E.; Ben-David, Y.; Milstein, D. *Angew. Chem., Int. Ed.* **2011**, *50*, 11702−11705.
(38) Tanaka, R.; Yamashita, M.; Nozaki, K. *J. Am. Chem. Soc.* **2011**, *131*, 14168−14169.
(39) Tanaka, R.; Yamashita, M.; Chung, L. W.; Morokuma, K.; Nozaki, K. *Organometallics* **2011**, *30*, 6742−6750.
(40) Langer, R.; Diskin-Posner, Y.; Leitus, G.; Shimon, L. J. W.; Ben-David, Y.; Milstein, D. *Angew. Chem., Int. Ed.* **2011**, *50*, 9948−9952.
(41) Huff, C. A.; Sanford, M. S. *J. Am. Chem. Soc.* **2012**, *133*, 18122−18125.
(42) Vogt, M.; Gargir, M.; Iron, M. A.; Diskin-Posner, Y.; Ben-David, Y.; Milstein, D. *Chem.-Eur. J.* **2012**, *18*, 9194−9197.
(43) Huff, C. A.; Kampf, J. W.; Sanford, M. S. *Organometallics* **2012**, *31*, 4643−4645.
(44) Vogt, M.; Rivada-Wheelaghan, O.; Iron, M. A.; Leitus, G.; Diskin-Posner, Y.; Shimon, L. J. W.; Ben-David, Y.; Milstein, D. *Organometallics* **2013**, *32*, 300−308.

(45) Montag, M.; Zhang, J.; Milstein, D. *J. Am. Chem. Soc.* **2012**, *134*, 10325−10328.
(46) Ozerov, O. V.; Watson, L. A.; Pink, M.; Caulton, K. G. *J. Am. Chem. Soc.* **2007**, *129*, 6003−6016.
(47) Michos, D.; Luo, X. L.; Crabtree, R. H. *J. Chem. Soc., Dalton Trans.* **1992**, 1735−1738.
(48) Marchi, A.; Marvelli, L.; Rossi, R.; Magon, L.; Uccelli, L.; Bertolasi, V.; Ferretti, V.; Zanobini, F. *J. Chem. Soc., Dalton Trans.* **1993**, 1281−1286.
(49) Bolzati, C.; Boschi, A.; Uccelli, L.; Tisato, F.; Refosco, F.; Cagnolini, A.; Duatti, A.; Prakash, S.; Bandoli, G.; Vittadini, A. *J. Am. Chem. Soc.* **2002**, *124*, 11468−11479.
(50) Bolzati, C.; Benini, E.; Cazzola, E.; Jung, C.; Tisato, F.; Refosco, F.; Pietzsch, H. J.; Spies, H.; Uccelli, L.; Duatti, A. *Bioconjugate Chem.* **2004**, *15*, 628−637.
(51) Porchia, M.; Tisato, F.; Refosco, F.; Bolzati, C.; Cavazza-Ceccato, M.; Bandoli, G.; Dolmella, A. *Inorg. Chem.* **2005**, *44*, 4766−4776.
(52) Kim, Y. S.; He, Z.; Hsieh, W. Y.; Liu, S. *Bioconjugate Chem.* **2006**, *17*, 473−484.
(53) Choualeb, A.; Lough, A. J.; Gusev, D. G. *Organometallics* **2007**, *26*, 3509−3515.
(54) Lang, H.-F.; Fanwick, P. E.; Walton, R. A. *Inorg. Chim. Acta* **2002**, *329*, 1−8.
(55) Kuang, S.-M.; Fanwick, P. E.; Walton, R. A. *Inorg. Chem.* **2002**, *41*, 405−412.
(56) Landwehr, A.; Dudle, B.; Fox, T.; Blacque, O.; Berke, H. *Chem.-Eur. J.* **2012**, *18*, 5701−5714.
(57) Jiang, Y.; Hess, J.; Fox, T.; Berke, H. *J. Am. Chem. Soc.* **2010**, *132*, 18233−18247.
(58) Dudle, B.; Rajesh, K.; Blacque, O.; Berke, H. *J. Am. Chem. Soc.* **2011**, *133*, 8168−8178.
(59) Jiang, Y.; Schirmer, B.; Blacque, O.; Fox, T.; Grimme, S.; Berke, H. *J. Am. Chem. Soc.* **2013**, *135*, 4088−4102.
(60) Schleker, P. P. M.; Honeker, R.; Klankermayer, J.; Leitner, W. *ChemCatChem* **2013**, *5*, 1762−1764.
(61) Lewis, R. A.; Wu, G.; Hayton, T. W. *Inorg. Chem.* **2013**, *50*, 4660−4668.
(62) Lewis, R. A. R.; Wu, G. G.; Hayton, T. W. T. *J. Am. Chem. Soc.* **2010**, *132*, 12814−12816.
(63) Soriaga, R. A. D. R.; Nguyen, J. M. J.; Albright, T. A. T.; Hoffman, D. M. D. *J. Am. Chem. Soc.* **2010**, *132*, 18014−18016.
(64) Lewis, R. A.; George, S. P.; Chapovetsky, A.; Wu, G.; Figueroa, J. S.; Hayton, T. W. *Chem. Commun.* **2013**, *49*, 2888−2890.
(65) Seaman, L. A.; Wu, G.; Edelstein, N.; Lukens, W. W.; Magnani, N.; Hayton, T. W. *J. Am. Chem. Soc.* **2012**, *134*, 4931−4940.
(66) Kiplinger, J. L.; Morris, D. E.; Scott, B. L.; Burns, C. J. *Organometallics* **2002**, *21*, 3073−3075.
(67) Lewis, R. A.; Morochnik, S.; Chapovetsky, A.; Wu, G.; Hayton, T. W. *Angew. Chem., Int. Ed.* **2012**, *51*, 12772−12775.
(68) Ferreira, M. J.; Martins, A. M. *Coord. Chem. Rev.* **2006**, *250*, 118−132.
(69) Henderson, K. W.; Hind, A.; Kennedy, A. R.; McKeown, A. E.; Mulvey, R. E. *J. Organomet. Chem.* **2002**, *656*, 63−70.
(70) Martins, A. M.; Marques, M. M.; Ascenso, J. R.; Dias, A. R.; Duarte, M. T.; Fernandes, A. C.; Fernandes, S.; Ferreira, M. J.; Matos, I.; Conceição Oliveira, M.; Rodrigues, S. S.; Wilson, C. *J. Organomet. Chem.* **2005**, *690*, 874−884.
(71) Ferreira, M. J.; Matos, I.; Ascenso, J. R.; Duarte, M. T.; Marques, M. M.; Wilson, C.; Martins, A. M. *Organometallics* **2007**, *26*, 119−127.
(72) The $^{1}$H NMR spectrum at −65 °C in toluene-$d_8$ has three distinct resonances for the $CH_3$ groups of the P−$^{t}$Bu moiety in vicinity to the axial ketimido nitrogen atom. Broad peaks integrating to three protons are found for the methyl groups at −0.38 ppm (br, d, $^{3}J_{HP}$ = 16.5 Hz), 0.92 ppm (br, s), and 1.95 ppm (br, d, $^{3}J_{HP}$ = 10.7 Hz). We hypothesize that this splitting into three resonances is due to hindrance of the free rotation of the P−$^{t}$Bu group upon [1,3]-addition of the pivalonitrile to **4**. The other resonances for the P−$^{t}$Bu groups are observed as doublets ($^{3}J_{HP}$ = 11.0 Hz) at 1.54 and 1.44 ppm, and a broad singlet at 1.19 ppm with integration equal to nine protons each.
(73) Scepaniak, J. J.; Wu, G.; Hayton, T. W. *Dalton Trans.* **2012**, *41*, 7859−7861.
(74) Soriaga, R. A. D.; Javed, S.; Hoffman, D. M. *J. Cluster Sci.* **2010**, *21*, 567−575.
(75) Upon cooling a solution of **8** in toluene-$d_8$, a second minor (10% at −65 °C) species is detected. The $^{31}$P{$^{1}$H}NMR shows an AB-spin system with large separation of the two doublets at 86.4 and 125.8 ppm ($^{2}J_{PP}$ = 194.0 Hz) typically observed for the ketimido complexes (e.g., the analogue complex **7**). However, a reliable assignment of the NMR data to such a species could not be made with certainty due to overlapping NMR resonances.
(76) Goto, M.; Ishikawa, Y.; Ishihara, T.; Nakatake, C.; Higuchi, T.; Kurosaki, H.; Goedken, V. *J. Chem. Soc., Dalton Trans.* **1998**, 1213−1222.
(77) Goto, M.; Ishikawa, Y.; Ishihara, T.; Nakatake, C.; Higuchi, T.; Kurosaki, H.; Goedken, T. L. V. L. *Chem. Commun.* **1997**, 539−540.
(78) Kurosaki, H.; Ishikawa, Y.; Ishihara, T.; Yamamoto, T.; Yamaguchi, Y.; Goto, M. *Dalton Trans.* **2005**, 1086−1092.
(79) Selva, M.; Marques, C. A.; Tundo, P. *J. Chem. Soc., Perkin Trans. 1* **1994**, 1323.
(80) Selva, M.; Perosa, A. *Green Chem.* **2008**, *10*, 457−464.
(81) The double addition product **14** is observed in low concentration (<10%) at the end of the reaction of benzyl cyanide and methyl acrylate in 1:1 ratio to form **13** (see GC traces in the Supporting Information). The first Michael addition step to form **13** proceeds more selectively under milder conditions (65 °C, 1:1 ratio). Hence, the first Michael addition is considerably faster than the second. The double addition product was obtained upon stepwise addition of benzyl cyanide or starting from a 1:2 ratio at higher temperature (80 °C). A control experiment has shown that catalytic amounts of KO$^{t}$Bu catalyze the Michael addition between benzyl cyanide and methyl acrylate. However, a significantly lower selectivity for the monoaddition product **13** was observed; see GC traces and Supporting Information Table S1 in the Experimental Section.
(82) Shimizu, S.; Shirakawa, S.; Suzuki, T.; Sasaki, Y. *Tetrahedron* **2001**, *57*, 6169−6173.
(83) Hermann, D.; Gandelman, M.; Rozenberg, H.; Shimon, L. J. W.; Milstein, D. *Organometallics* **2002**, *21*, 2−818.
(84) Frisch, M. J.; Trucks, G. W.; Schlegel, H. B.; Scuseria, G. E.; Robb, M. A.; Cheeseman, J. R.; Scalmani, G.; Barone, V.; Mennucci, B.; Petersson, G. A.; Nakatsuji, H.; Caricato, M.; Li, X.; Hratchian, H. P.; Izmaylov, A. F.; Bloino, J.; Zheng, G.; Sonnenberg, J. L.; Hada, M.; Ehara, M.; Toyota, K.; Fukuda, R.; Hasegawa, J.; Ishida, M.; Nakajima, T.; Honda, Y.; Kitao, O.; Nakai, H.; Vreven, T.; Montgomery, J. A., Jr.; Peralta, J. E.; Ogliaro, F.; Bearpark, M.; Heyd, J. J.; Brothers, E.; Kudin, K. N.; Staroverov, V. N.; Kobayashi, R.; Normand, J.; Raghavachari, K.; Rendell, A.; Burant, J. C.; Iyengar, S. S.; Tomasi, J.; Cossi, M.; Rega, N.; Millam, J. M.; Klene, M.; Knox, J. E.; Cross, J. B.; Bakken, V.; Adamo, C.; Jaramillo, J.; Gomperts, R.; Stratmann, R. E.; Yazyev, O.; Austin, A. J.; Cammi, R.; Pomelli, C.; Ochterski, J. W.; Martin, R. L.; Morokuma, K.; Zakrzewski, V. G.; Voth, G. A.; ,Salvador, P.; Dannenberg, J. J.; Dapprich, S.; Daniels, A. D.; Farkas, O.; Foresman, J. B.; Ortiz, J. V.; Cioslowski, J.; Fox, D. J. *Gaussian 09*, revision C.01; Gaussian, Inc.: Wallingford, CT, 2009.
(85) Perdew, J. P.; Burke, K.; Ernzerhof, M. *Phys. Rev. Lett.* **1996**, *77*, 3865−3868.
(86) Perdew, J. P.; Burke, K.; Ernzerhof, M. *Phys. Rev. Lett.* **1997**, *78*, 1396.
(87) Kozuch, S.; Martin, J. M. L. *Phys. Chem. Chem. Phys.* **2011**, *13*, 20104−20107.
(88) Adamo, C.; Barone, V. *J. Chem. Phys.* **1999**, *110*, 6158−6170.
(89) Perdew, J. *Phys. Rev. B: Condens. Matter* **1986**, *33*, 8822−8824.
(90) Szabados, A. *J. Chem. Phys.* **2006**, *125*, 214105.
(91) Grimme, S. *J. Chem. Phys.* **2003**, *118*, 9095−9102.
(92) Møller, C.; Plesset, M. S. *Phys. Rev.* **1934**, *46*, 618−622.
(93) Grimme, S.; Antony, J.; Ehrlich, S.; Krieg, H. *J. Chem. Phys.* **2010**, *132*, 154104.

(94) Schwabe, T.; Grimme, S. *Acc. Chem. Res.* **2008**, *41*, 569−579.
(95) Schwabe, T.; Grimme, S. *Phys. Chem. Chem. Phys.* **2007**, *9*, 3397−3406.
(96) Grimme, S. *J. Comput. Chem.* **2006**, *27*, 1787−1799.
(97) Grimme, S.; Ehrlich, S.; Goerigk, L. *J. Comput. Chem.* **2011**, *32*, 1456−1465.
(98) Johnson, E. R.; Becke, A. D. *J. Chem. Phys.* **2006**, *124*, 174104.
(99) Dunning, T. H., Jr.; Hay, P. J. In *Modern Theoretical Chemistry 3. Methods of Electronic Structure Theory*; Schaefer, H. F., III, Ed.; Plenum Press: New York, 1976; Vol. *3*, pp 1−28.
(100) Dolg, M. In *Modern Methods and Algorithms of Quantum Chemistry*; Grotendorst, J., Ed.; John von Neumann Institute for Computing: Jülich, 2000; Vol. *3*, pp 507−540.
(101) Dunning, T. H., Jr. *J. Chem. Phys.* **1989**, *90*, 1007−1023.
(102) Wilson, A. K.; Woon, D. E.; Peterson, K. A.; Dunning, T. H., Jr. *J. Chem. Phys.* **1999**, *110*, 7667−7676.
(103) Peterson, K. A.; Figgen, D.; Dolg, M.; Stoll, H. *J. Chem. Phys.* **2007**, *126*, 124101.
(104) Dunlap, B. I. *J. Chem. Phys.* **1983**, *78*, 3140−3142.
(105) Dunlap, B. I. *J. Mol. Struct. (THEOCHEM)* **2000**, *529*, 37−40.
(106) Mennucci, B.; Tomasi, J. *J. Chem. Phys.* **1997**, *106*, 5151−5158.
(107) Cancès, E.; Mennucci, B.; Tomasi, J. *J. Chem. Phys.* **1997**, *107*, 3032−3041.
(108) Cossi, M.; Barone, V.; Mennucci, B.; Tomasi, J. *Chem. Phys. Lett.* **1998**, *286*, 253−260.
(109) Cossi, M.; Scalmani, G.; Rega, N.; Barone, V. *J. Chem. Phys.* **2002**, *117*, 43−54.
(110) Mennucci, B.; Cancès, E.; Tomasi, J. *J. Phys. Chem. B* **1997**, *101*, 10506−10517.
(111) Tomasi, J.; Mennucci, B.; Cancès, E. *J. Mol. Struct. (THEOCHEM)* **1999**, *464*, 211−226.
(112) Marenich, A. V.; Cramer, C. J.; Truhlar, D. G. *J. Phys. Chem. B* **2009**, *113*, 6378−6396.